

# EPSC2017

## **MT6 abstracts**

# New Release of the High-Resolution Mimas Atlas derived from Cassini-ISS Images

Th. Roatsch(1), E. Kersten(1), K.-D. Matz(1), and C.C. Porco(2)

(1) Institute of Planetary Research, German Aerospace Center (DLR), Berlin, Germany, (2) CICLOPS, Space Science Institute, Boulder, CO ([Thomas.Roatsch@dlr.de](mailto:Thomas.Roatsch@dlr.de))

## 1. Introduction

The Cassini Imaging Science Subsystem (ISS) acquired 128 high-resolution images (< 1 km/pixel) of Mimas during its tour through the Saturnian system since 2004. We combined new images from orbit 249 (Nov. 2016) and orbit 259 (Jan. 2017) with the high-resolution global semi-controlled mosaic of Mimas from 2012. This global mosaic is the baseline for the new high-resolution Mimas atlas that still consists of three tiles mapped at a scale of 1:1,000,000 [1]. The nomenclature used in this atlas was proposed by the Cassini imaging team and was approved by the International Astronomical Union (IAU). The entire atlas will become available to the public through the Imaging Team's website [<http://ciclops.org/maps>] and the Planetary Data System (PDS) [<https://pds-imaging.jpl.nasa.gov/volumes/carto.html>].

## 2. Data Processing

The image data processing chain consists of the same steps as described in [2]: radiometric calibration, geometric correction, map projection, and mosaicking. Spacecraft position and camera pointing data are available in the form of SPICE kernels [<http://naif.jpl.nasa.gov>]. While the orbit information is sufficiently accurate to be used directly for mapping purposes, the pointing information must be corrected using limb fits. The coordinate system adopted by the Cassini mission for satellite mapping is the IAU “planetographic” system,

consisting of planetographic latitude and positive West longitude. The surface position of the prime meridian as defined by the IAU cartography working group [3] is defined by the small crater Palomides.

## 3. Mimas map tiles

The Mimas atlas was produced in a scale of 1:1,000,000 and consists of three tiles that conform to the quadrangle scheme proposed by Greeley and Batson [4]. In 2008 the Cassini imaging team proposed 6 names for geological features, in addition to the 36 features already named by the Voyager team that are used in the maps. By international agreement, the features must be named after people or places from Malory's „Le Morte d'Arthur“ legends.

## Reference

- [1] Roatsch, T. et al., 2013, Recent improvements of the Saturnian satellites atlases: Mimas, Enceladus, and Dione, *Planetary and Space Science* 77, 118-125.
- [2] Roatsch, T. et al., 2006, Mapping of the icy Saturnian satellites: First results from Cassini-ISS, *Planetary and Space Science* 54, 1137-1145.
- [3] Archinal, B. et al., 2011, Report of the IAU Working Group on Cartographic Coordinates and Rotational Elements: 2009, *Celest. Mech. Dyn. Astr.* 109, 101-135
- [4] Greeley, R. and Batson, G., 1990, *Planetary Mapping*, Cambridge University Press

# 15 maps merged in one data structure - GIS-based template for Dawn at Ceres

A. Naß (1), and the Dawn Mapping Team

(1) DLR, Institute for Planetary Research, Rutherfordstrasse 2, 12489 Berlin, Germany (andrea.nass@dlr.de)

## Abstract

Derive regional and global valid statements out of the map (quadrangles) is already a very time intensive task. However, another challenge is how individual mappers can generate one homogenous GIS-based project (w.r.t. geometrical and visual character) representing one geologically-consistent final map.

## 1. Introduction

One aim of the NASA Dawn mission is to generate global geologic maps of the asteroid Vesta and the dwarf planet Ceres. The geological mapping campaign of Vesta was completed and published, e.g. [1], but mapping of Ceres is still ongoing. The tiling schema for the mapping project based on recommendations by [2], and is divided into two parts (for Ceres described in [3]): four overview quadrangles (Survey Orbit, 415 m/pixel) and 15 more detailed quadrangles (High Altitude Mapping HAMO, 140 m/pixel). The first global geologic map based on survey images [4]. This served as basis for generating a more detailed view of the geologic history and also for defining the chrono-stratigraphy and time scale of the dwarf planet [5]. The most detailed view can be expected within the 15 quadrangles based on HAMO resolution and completed by the Low Altitude Mapping (LAMO) data (35 m/pixel). For the interpretative mapping one responsible mapper was assigned for each quadrangle. Once the mapping is finished, all datasets must be combinable in ESRI's ArcGIS™.

Within this contribution a template will be presented which was generated for the process of the interpretative mapping project of Ceres to accomplish the requirement of unifying and merging individual quadrangle. The template

1. accommodates the requirements for data storage and database management (e.g., [6]),
2. uses standards for digitizing, visualization, data merging and synchronization,

3. based on new technological GIS innovations within GIS software and individual requirements for mapping Ceres, and
4. furthermore, on developments regarding symbology and framework described in [7], [8].

## 2. Mapping Template

The mapping template is based on the ArcGIS format file-geodatabase (FGDB) and split in three main layers: 1) basis data layer (bdl): as placeholder for the map-projected images, upon which the mapping based on, 2) map sheet layer (msl): includes map graticules and the different quadrangle boundaries and 3) geologic mapping layer (gml): contains the layers for vector-based mapping all planetary features. Beside this the FGDB structure includes (a) 5 *feature classes* representing specific types of geologic features (all vector based), (b) *subtypes and domains* are hierarchical, or domain-controlled, attributes that are coordinated within each main layer, (c) *cartographic symbols* follow [9] as far as possible, and (d) *speciality*: the colours for the geological units were defined by individual needs and requests within the mapping team. The colour choice was based on established colour values used in geologic maps, e.g., generated by USGS.

Furthermore, the mappers were supported by (e) *instruction documents*, (f) a *metadata template* based on standardized metadata keywords, e.g., defined in [10], [11], and (g) *extra template* arrange all map components (legend, map title, grid, projection information etc.) uniformly in a predefined map sheet (usable in vector-based software).

## 3. Review and Open Questions

The mapping template has served as a necessary basis for the mappers to generate their individual but comparable maps, and thus gives the possibility to merge 15 quads to one global map (see figure 1). The current status and general information of the mapping project are summarized in [12]. Because the creation of the mapping template was and is an iterative

process which is still in progress, there are still some topics (focus on GIS and cartographic visualization) to discuss on the way to a homogenous and comparable map layout. These are, e.g., the *boundary regions* of all quads have to be strongly reviewed to enable a consistent description of Ceres, regarding the individual *colour scheme* it has to decide very carefully if additional colours for individual and regional phenomena should be used, and an updated version of the already existing *feature catalogue* (by Katrin Krohn, DLR) and the generated *global map legend* could be *combined* to describe the different features generically and visually. This would provide a first global view of the objects and units on Ceres and could be used for more detailed investigation.

## 4. Summary

The template for (GIS-base) mapping presented here directly links the generically descriptive attributes of planetary objects to the predefined and standardized symbology in one data structure. Using this template the map results are more comparable and controllable. Merge and synchronize the individual maps will be far more efficient, and first possible. The template can be adapted to other planetary body, is also useable in open source software QGIS and could be transfer to database systems like PostgreSQL, and/or

be used within future discovery missions (e.g., Lucy and Psyche) for generating reusable map results.

## Acknowledgements

This work is supported by E. Kersten (DLR, Berlin), David Nelson (ASU) and the Dawn Mapping Team. Furthermore by the valuable discussions with and the efforts taken by Stephan van Gasselt (University Seoul) and the USGS Astrogeology Science Centre, Flagstaff.

## References

- [1] Greeley, R. & Batson, G., *Planetary Mapping*, Cambridge University Press, 1990
- [2] Williams D.A. et al. *Icarus*, 244, 1-12, 2014
- [3] Roatsch, T. et al., *PSS* 129, 103-107, 2016
- [4] Buczkowski, D.L. et al., *Science* 353, 2016,
- [5] Mest, S. et al., *LPSC 2017*, #2512, 2017.
- [6] Arctur, D. & Zeiler, M., *Designing Geodatabases*, ESRI Press, Redlands, CA., 2004
- [7] Naß, A. et al., *PSS* 59(11-12), 2011.
- [8] van Gasselt, S. & Naß, A., *PSS* 59(11-12), 2011,
- [9] FGDC, *Digital Cartographic Standard for Geologic Map Symbolization*, FGDC-STD-013-2006, 2006,
- [10] PDS *Planetary Data System Standard Reference*, Technical Report. 2009,
- [11] FGDC, *Content Standard for Digital Geospatial Metadata (Workbook)*, FGDC-STD-001-1998, 1998, 2000
- [12] Williams, D.A. et al., *LPSC 2017* #1451, 2017.

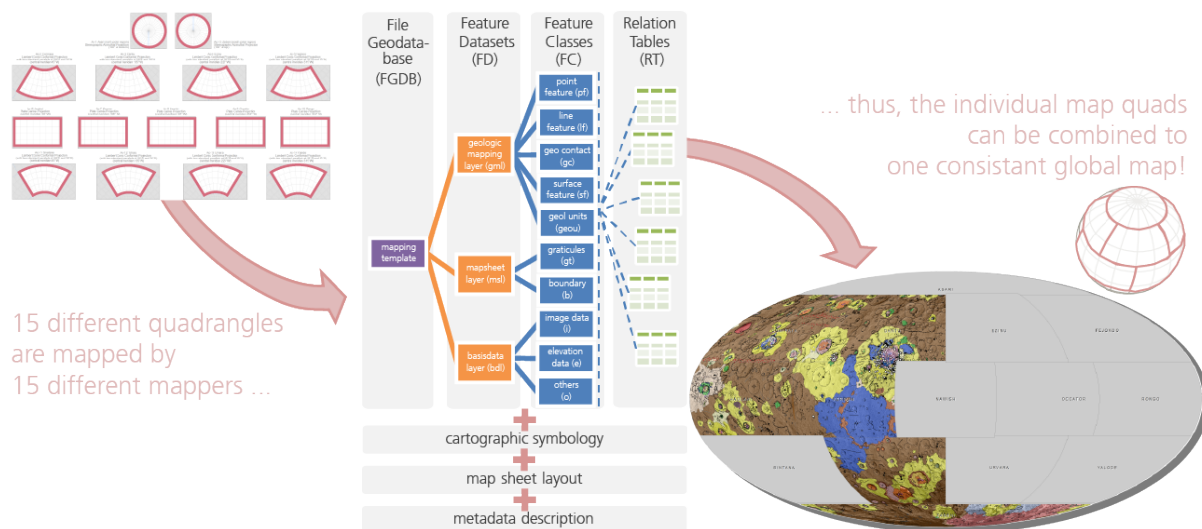


Figure 1: Schematic view on file geodatabase-driven Geological Mapping Template for Ceres.



## Digital Geologic Mapping of Vesta and Ceres from NASA's Dawn Mission

D.A. Williams (1), S.C. Mest (2), D.L. Buczkowski (3), J.E.C. Scully (4), and the NASA Dawn Science Team.  
(1) School of Earth & Space Exploration, Arizona State University, Tempe, AZ, USA, [David.Williams@asu.edu](mailto:David.Williams@asu.edu); (2) Planetary Science Institute, Tucson, AZ, USA; (3) Applied Physics Laboratory, Johns Hopkins University, Laurel, MD, USA, (4) NASA Jet Propulsion Laboratory, California Institute of Technology, Pasadena, CA, USA.

### Abstract

NASA's Dawn mission [1] was designed to orbit the two most massive objects in the Main Asteroid Belt, asteroid 4 Vesta and dwarf planet 1 Ceres. Dawn successfully accomplished her mission at Vesta in 2011-2012 and at Ceres in 2015-2017, including several orbital phases at each object where increasingly higher spatial resolution data were obtained. These data facilitated iterative digital geological mapping of both objects, including production of global geologic maps and a series of quadrangle maps. In this presentation we describe the details of the Vesta and Ceres Mapping Campaigns and key results obtained for both objects.

### Approach

1. Geologic mapping is an investigative process that goes beyond photogeologic analysis by organizing planetary features into discrete process-related map units. These units are defined and characterized based on specific physical attributes (albedo, morphology, structure, color, topography) related to the putative geologic processes that produced them (volcanism, tectonism, impact cratering, weathering-erosion-deposition). Application of stratigraphic principles (superposition, lateral continuity, cross-cutting, embayment, intrusion, etc.) are used to determine the chronologic order of emplacement of the map units. The map units can then be grouped into geologic formations, from which a geologic timescale and geologic history is determined. Thus, geologic maps are *tools* to help interpret the geologic history of a planetary surface.

2. The geologic mapping approach was similar for both Vesta and Ceres. The Dawn Science Team requested geologic mapping campaigns with the goals to: a) Identify the variety and stratigraphic correlations of geologic features on these two objects, and b) Provide geologic context for the interpretation of compositional measurements from the Visible and Infrared Spectrometer (VIR) and Gamma Ray and Neutron Detector (GRaND). The geologic mapping was iterative, using increasingly higher spatial

resolution Framing Camera (FC) image mosaics obtained by the various orbital phases at each object: Approach, Survey, High Altitude Mapping Orbit (HAMO), Low Altitude Mapping Orbit (LAMO). A global geologic map was produced from the HAMO mosaics, and a series of 15 quadrangle maps were made from the LAMO mosaics. The mosaics, along with corresponding digital terrain models (DTMs, made using stereo photogrammetry) were produced by the German Aerospace Center (DLR) to support Science Team activities. Geologic mapping was done using ArcGIS™ software, and the mapping team met regularly at Team Meetings to correlate geologic units and contacts across quadrangle boundaries. For the Ceres campaign, a dedicated technician with background in ArcGIS was brought onboard to facilitate digital geologic map production.

### Vesta Geologic Mapping Campaign

3. The HAMO-based global geologic map of Vesta was published by [2], the LAMO-based quadrangle maps were published in the December 2014 issue of *Icarus* [3] including the vestan chronostratigraphy and geologic timescale [4]. A new unified quadrangle, LAMO global geologic was presented by [5], and currently production of a U.S. Geological Survey-publishable global geologic map of Vesta is underway.

4. Globally, impact cratering has dominated the geologic evolution of Vesta. Ancient impacts have constrained the structure of the surface, and later impacts have influenced the distribution of ejecta and exposure of volatiles. Almost all evidence of the ancient volcanic processes implied by the Howardite-Eucrite-Diogenite (HED) meteorites has been completely destroyed – only one dome-like feature, Brumalia Tholus, interpreted as a laccolith, hints at Vesta's igneous past [6]. Brumalia Tholus occurs on Vestalia Terra, a relatively high-standing terrain which superposition relations suggests is the last remaining part of Vesta's original crust [6] and gravity data suggests might be a fossil mantle plume [7]. The Veneneia and Rheasilvia impact basins at Vesta's south pole produced a set of northern latitude

and equatorial ridge-and-trough systems, respectively, that cover large segments of the surface. These fossae systems are thought to be a tectonic response to the formation of the south polar basins [8]. Pitted terrain has been identified in several craters [9], which along with curvilinear gully systems in several crater interiors [10] suggest the presence of volatiles (perhaps water ice) scattered within the vestan crust. Lobate deposits demonstrate the role of mass wasting and impact melt in the modification of the surface.

## Ceres Geologic Mapping Campaign

5. The HAMO-based global geologic map of Ceres is completed (**Figure 1**) and a manuscript is in preparation. The LAMO-based quadrangle maps are currently under peer review for publication in a special issue of *Icarus* hopefully for late 2017.

6. Global map units include ancient cratered terrain, smooth material, younger crater materials, lobate materials, rayed crater material, among others. Formations separate the Yalode and Urvara impact

units that dominate the southern hemisphere. The 284-km diameter Kerwan basin is the oldest crater on Ceres, and separates Pre-Kerwanan cratered terrain from younger Urvaran and Yalodean units. The youngest materials on Ceres (Azaccan) define the era of rayed craters (as does the Copernican on the Moon), and includes most recognized mass wasting, glacial-like, and cryovolcanic flows.

## References:

- [1] Russell, C.T., and Raymond, C.A., 2012, *Space Sci. Rev.*, 163, 3-23; [2] Yingst, R.A., et al., 2014, *Planet. Space Sci.*, 103, 2-23; [3] Williams, D.A., et al., 2014, *Icarus*, 244, 1-12; [4] Williams, D.A., et al., 2014, *Icarus*, 244, 158-165; [5] Williams, D.A., et al., 2015, *LPSC XLVI*, Abstract #1126, LPI, Houston (PDF); [6] Buczkowski et al., 2014, *Icarus*, doi: 10.1016/j.icarus.2014.03.035; [7] Raymond, C.A., et al., 2017, Ch. 15, in *Planetesimals*, Camb. Un. Press, 321-340; [8] Buczkowski, D.L., et al., 2012, *GRL* 39, L18205, doi:10.1029/2012GL052959; [9] Denevi, B.W., et al., 2012, *Science*, 338, 246-249; [10] Scully, J. E. C., et al., 2015, *EPSL* 411, 151-163.

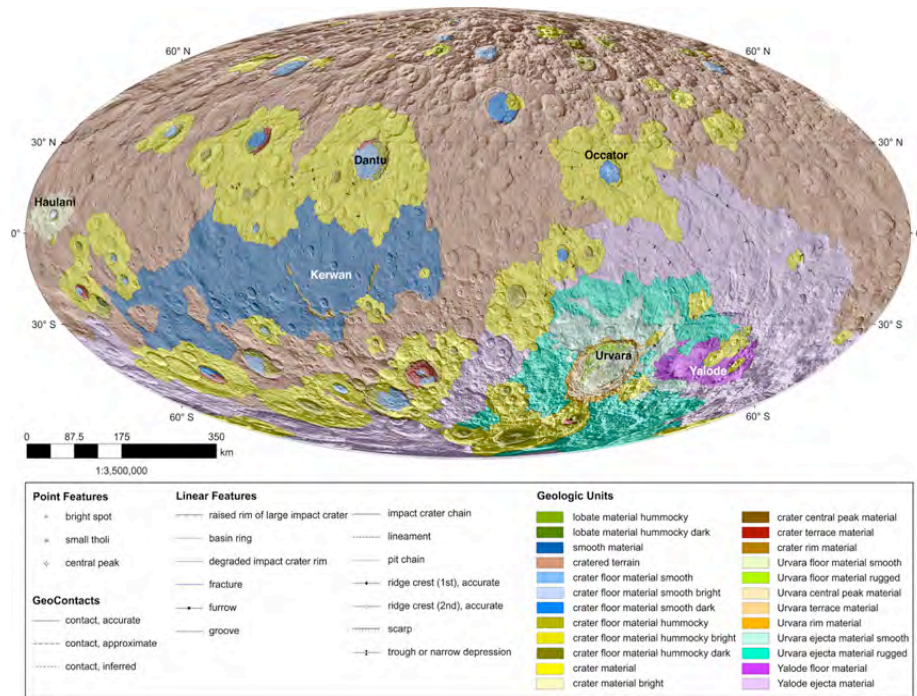


Figure 1. HAMO-based global geologic map of Ceres, scale 1:3.5M. Mapping by Scott Mest, PSI.

# Geologic Mapping of Ascræus Mons, Mars

**K. J. Mohr** (1), D. A. Williams (1), W. B. Garry (2), and J. E. Bleacher (2)

(1) School of Earth & Space Exploration, Arizona State University, Tempe, AZ 85282, (kyle.mohr@asu.edu), (2) Geology, Geophysics, and Geochemistry Laboratory, Code 698, NASA Goddard Space Flight Center, Greenbelt, MD 20771.

## Abstract

New mapping of Ascræus Mons on Mars using higher resolution imagery has allowed for a more dynamic understanding of the complex history of building the large shield volcano and the surrounding Tharsis Province.

## 1. Introduction/Background

Ascræus Mons (AM) is the northeastern most large shield volcano residing in the Tharsis province on Mars. We are funded by NASA's Mars Data Analysis Program to complete a digital geologic map based on the mapping style defined by [1,2]. Previous mapping of a limited area of these volcanoes using HRSC images (13-25 m/pixel) revealed a diverse distribution of volcanic landforms within the calderas, along the flanks, rift aprons, and surrounding plains [1,4]. The general scientific objective for which this mapping is based is to show the different lava flow morphologies across AM to better understand the evolution and geologic history.

## 2. Data and Methods

We have finished geologic mapping of Ascræus Mons at a 1:1,000,000 scale using ArcMap 10.3. A CTX mosaic and a THEMIS daytime IR mosaic were used as the primary basemaps, supplemented by HRSC, HiRISE, and MOLA data.

The THEMIS daytime IR mosaic was used to look at larger scale structures on the flanks, rift aprons, and plains surrounding AM. Once an area of interest was found using the THEMIS mosaic we used the CTX mosaic and supplemental images to look at smaller scale features, such as: surface textures, contacts, depressions, collapse features, small lava flows, erosional features, aeolian deposits, and tectonics. Where CTX images were poor we supplemented with HRSC and HiRISE images. All images and mosaics were tied together with MOLA data to determine accurate points of reference.

Contacts and linear features were mapped generally using CTX data, this allowed for the best visual scale for the 1:1M mapping scale for the finished map product. Contacts and geologic units were defined by looking at the morphology of the surface on the flanks, rift aprons, and plains of AM.

Linear features were mapped first, followed by contacts, then surface features, and lastly geologic units.

## 3. Geologic Observations

A total of 27 units have been observed on the flanks, rift aprons, and the surrounding plains; some of these units have facies changes, but are lumped together to best fit the 1:1,000,000 mapping scale.

### 3.1. Main Shield

The main shield (labeled as *Flank* in the legend, Fig. 1) has been divided into 9 different units which includes the large summit caldera complex, collapsed features, such as depressions, channel-fed flows, raised ridges, impact crater cavities, and crater ejecta. The flanks of the shield are dominated by a mottled (Afm) unit surrounding the caldera and channel-fed flows (Afm), which cover the majority of the main shield.

### 3.2. Rift Apron

Ascræus Mons has two large rift aprons on the NE and SW flanks (Fig. 1). These rift aprons are the main source for the large amount of lava flows seen on the plains surrounding AM and have been divided into 7 different units: channel (Aac), muted (Aam), knobby (Aak), smooth (Aas), undifferentiated (Aau), and ridged (Aar, Aarm). The channel and ridged apron units are comparable to the channel-fed and ridged units found on the main shield. The muted apron is heavily mantled by dust and is typically located off the SW flank.

### 3.3. Plains

The plains surrounding Ascræus Mons have been subdivided into 6 units: aureole (AHpa), mottled (Apm), tabular (Apt), channel-fed (Apc), fissure-fed (Apf), and low shield (Apls). The Aureole unit is divided up into three separate units. The mottled and channel-fed units are characterized by the same distinctions found on the main shield and rift apron units.

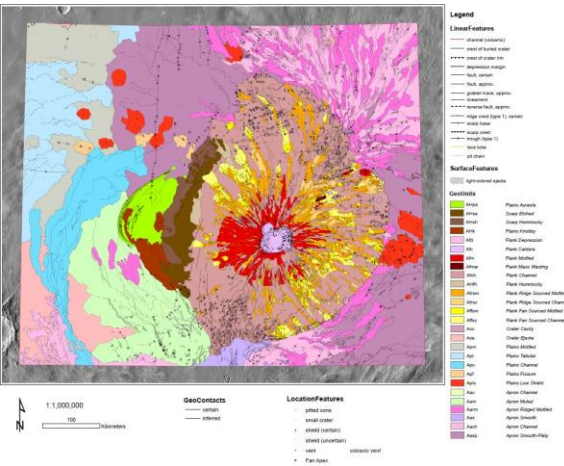


**Figure 1. Geologic map of Ascræus Mons, Mars at 1:1M scale.**

### 4. Summary and Conclusions

Mapping reveals a similar sequence of events for the evolution of Ascræus Mons that agrees with [1,2,3,4]: 1) main shield forms, 2) eruptions from the NE/SW rifts emplace long lava flows that surround main shield, 3) eruptions wane and build up the rift aprons and shield fields, 4) glaciers deposit aureole unit material, and 5) localized recent eruptions along the main flanks, in the calderas, the small-vent field, and possibly within the glacial aureole deposits. Higher resolution images allow for a better understanding of the evolution of the large shield volcano. Whereas previously very few map units were observed, now 27 map units can be found to show the dynamic evolution of Ascræus Mons and give new insights into the history of the Tharsis Province on Mars.

### Acknowledgements

We thank NASA’s Mars Data Analysis Program, grant number NNX14AM30G for funding the research of this project as well as the staff at the Ronald Greeley Center for Planetary Studies for their hardwork and cooperation in helping to see this project become completed.

### References

[1] Bleacher J. E. et al. (2007) JGR, 112, E04003, doi:10.1029/2006JE002826.

[2] Bleacher J. E. et al. (2007) JGR, 112, E09005, doi:10.1029/2006JE002873.

[3] Crumpler L. S. and Aubele J. C. (1978) *Icarus*, 34, 496-511.

[4] Garry W. B. et al. (2014) LPSC 45, #2133.



# Creating a Road Map for Planetary Data Spatial Infrastructure

A. Naß(1), B. Archinal(2), R. Beyer(3), D. DellaGiustina(4), C. Fassett(5), L. Gaddis(2), J. Hagerty(2), T. Hare(2), J. Laura(2), S. Lawrence(6), E. Mazarico(7), A. Patthoff(8), J. Radebaugh(9), J. Skinner(2), S. Sutton(4), B. J. Thomson(10), D. Williams(11); (1) DLR, Berlin, Germany (andrea.nass@dlr.de), (2) USGS, Flagstaff, AZ, USA, (3) SETI/NASA/Ames, Mountain View, CA, USA, (4) Univ. of Arizona, Tucson, AZ, USA, (5) NASA/MSFC, Huntsville, AL, USA, (6) NASA/JSC, Houston, TX, USA, (7) NASA/GSFC, Greenbelt, MD, USA, (8) PSI, Tucson, AZ, USA, (9) Brigham Young Univ., Provo, UT, USA, (10) Univ. of Tennessee, Knoxville, TN, USA, (11) Arizona State Univ., Tempe, AZ, USA.

## Abstract

There currently exists a clear need for long-range planning in regard to planetary spatial data and the development of infrastructure to support its use. Planetary data are the hard-earned fruits of planetary exploration, and the Mapping and Planetary Spatial Infrastructure Team (MAPSIT) mission is to ensure their availability for any conceivable investigation, now or in the future.

## 1. Introduction

Planetary spatial data, which include any remote sensing, in-situ data or derived products with sufficient positional information such that they can be associated with a planetary body, continue to rapidly increase in volume and complexity. Maintaining these data using accessible formats and standards for all scientists is essential for the success of past, present, and future planetary missions. The MAPSIT is a group of planetary community members tasked by the Planetary Science Subcommittee of the NASA Advisory Council and NASA Headquarters to identify and prioritize the infrastructural spatial data needs for research and analysis using NASA's past, current, and future planetary science missions.

## 2. Planetary Spatial Data and MAPSIT

The extraction of scientific knowledge from planetary mission data relies on several steps of refinement of the raw data from instruments. Two of the most important are (1) the conversion of raw output into physically meaningful units and (2) placing the data into a recognized spatial framework. Creating scientifically useful information is often a major research and development effort in itself. To

complete this process, goals need to be identified, missions need to be properly designed, and instruments need to be appropriately developed and calibrated. The software tools and content distribution platforms required for scientists to obtain, process, and analyze planetary mission data need continuing development and maintenance. For these reasons, community coordination and strategic planning, or "road mapping," for the use of planetary spatial data are essential for the success of planetary exploration.

To this end, NASA and the USGS have worked together to establish MAPSIT, which has steering committee membership (the authors of this abstract) drawing from many aspects of planetary spatial data expertise and Solar System bodies. MAPSIT's mission is to ensure that planetary spatial data are readily available for any scientific investigations, now or in the future. MAPSIT has several functions: (1) Provide community findings, in the form of a road map concerning the scientific rationale, objectives, technology, and long-range strategic priorities for planetary mapping [1] and spatial (including topographic) software development (e.g., [2]); (2) Encourage the development of standards for present and future planetary missions and research activities, coordinate systems, mapping, geologic mapping, cartographic methods and nomenclature; (3) Help define community needs for critical research and planetary mission infrastructure, particularly software tools and content delivery systems [e.g., 3], (4) Provide findings on the accuracy and precision required for spatial technologies and products; and (5) Coordinate and promote the registration of data sets from international missions with those from US missions to optimize their combined utility.

MAPSIT will help enable the broad spectrum of planetary spatial data and programmatic capabilities required to effectively achieve robotic precursor and human exploration of the Solar System. These include (but are not limited to) the science analysis of

planetary surfaces, the identification of safe landing sites, the down-selection of sample acquisition locations, hazard assessment, and the spatial characterization of in-situ resources [4, 5, 6].

### 3. Immediate Issues

There are numerous, high-priority issues that the MAPSIT-represented community is focused on addressing in the near future:

- How should the current, unprecedented influx of high-volume, planetary mission data (e.g., Mars Reconnaissance Orbiter, Lunar Reconnaissance Orbiter, MESSENGER) be geodetically controlled and integrated to enable science and operation of current and future missions?
- How should global, regional, and local topographic models be created from multiple data sets?
- What requirements should be developed for missions to follow during the formulation and definition stages to mitigate subsequent growth of costs?
- How can research and analysis programs support strategic development of mapping procedures for new and complex products?
- How should community input be obtained and used to prioritize product development on near-term time scales? What products should be considered foundational (meaning a base or data set that all other data should be registered too)? [7, 8]
- How can planetary spatial data products be used to enable and facilitate future human exploration and in-situ resource utilization? [9]
- When and how should geodetic analysis and mapping tools be developed and be tested for accuracy and usability?
- How can training in planetary spatial data be established or encouraged so that existing expertise is passed on to next-generation workers?

One example of in-depth assessment that MAPSIT can facilitate includes addressing the needs for software tools to process data from all missions, including the increasingly complex and vast data volumes of current and future missions. Such software needs include (1) faster and more robust matching between disparate data types, enabling new types of data fusion; (2) the ability to simultaneously adjust data from different platforms (e.g., orbital, descent, lander, and rover) and data types (e.g., images, radar, and altimetry); and (3) new tools to combine different methods for generating topographic information.

## 4. A New Strategic Plan

MAPSIT's first task is to synthesize a new cohesive road map or Planetary Geospatial Strategic Plan (PGSP). To build such a plan, MAPSIT will solicit broad stakeholder input through community surveys and town hall meetings, such as at the Lunar and Planetary Science Conference and at a MAPSIT community meeting in conjunction with the June 2017 Planetary Data Workshop. A partial goal is to recommend and prioritize the needed data products and infrastructural developments, following a process much like that of the Lunar Exploration Roadmap [10], the 2015 Small Bodies Assessment Group Goals Document [11] and in part the Outer Planets Assessment Group Roadmap for Ocean Worlds. The road map assumes that a Planetary Spatial Data Infrastructure (PSDI) [7] will be created, which – not a road map itself – will outline and define all aspects of planetary spatial data and lays out the needs, capabilities and tasks of the community. This builds on a similar document for Earth Sciences in the US, the National Spatial Data Infrastructure (NSDI) document [12]. It is envisioned that the roadmap will be a living document that evolves over time as milestones are met and the state of the art advances.

## 5. Conclusions

The planetary science community faces numerous issues relating to NASA strategic planetary spatial data infrastructure, particularly as the US and international partners aim to carry out ambitious planetary missions throughout the Solar System. By involving key stakeholders in the process and by inclusively building an active and productive community, MAPSIT will help NASA and international partners drive future discovery and innovation.

## References

- [1] Skinner et al. (2017) *Plant. Sci. Vis.* 2050, #8243. [2] Becker et al. (2017) *Plant. Sci. Vis.* 2050, #8218. [3] Hare, T.M., et al., 2017. PSS, DOI:10.1016/j.pss.2017.04.004. [4] Archinal et al. (2016) LPS XLVII, #2377. [5] Kirk (2016) LPS XLVII, #2151. [6] Milazzo et al. (2017) *Plant. Sci. Vis.* 2050, #8070 & #8132. [7] Laura et al. (2017) *Plant. Sci. Vis.* 2050, #8110. [8] Archinal et al. (2017) LPS XLVIII, #2286. [9] Wargo et al. (2013) IAC 64, IAC-13-A3.1.4. [10] LEAG (2016) The Lunar Exploration Roadmap, <http://www.lpi.usra.edu/leag/roadmap>. [11] SBAG (2016) SBAG Goals Document, <http://www.lpi.usra.edu/sbag/goals>. [12] OMB (2002) NSDI, Circular No. A-16 Revised.



# The iMars web-GIS – spatio-temporal data queries and single image web map services

**S. H. G. Walter** ([s.walter@fu-berlin.de](mailto:s.walter@fu-berlin.de)) (1), R. Steikert (1), B. Schreiner (1), P. Sidiropoulos (2), Y. Tao (2), J.-P. Muller (2), A. R. D. Putry (2), S. van Gasselt (3)

(1) Institute for Geological Sciences, Freie Universitaet Berlin, Germany, (2) Mullard Space Science Laboratory, University College London, United Kingdom, (3) Department of Geo-Informatics, University of Seoul, Korea

## Introduction

Web-based planetary image dissemination platforms usually show outline coverages of the data and offer querying for metadata as well as preview and download, e.g. [1]. Here we introduce a new approach for a system dedicated to planetary surface change detection by simultaneous visualisation of single-image time series in a multi-temporal context. While the usual form of presenting multi-orbit datasets is to merge the data into a larger mosaic, we want to stay with the single image as an important snapshot of the planetary surface at a specific time. In the context of the EU FP-7 iMars project we process and ingest vast amounts of automatically co-registered (ACRO) images [2]. The base of the co-registration are the high precision HRSC multi-orbit quadrangle image mosaics [3], which are based on bundle-block-adjusted multi-orbit HRSC DTMs [4]. Additionally we make use of the existing bundle-adjusted HRSC single images available at the PDS archives [5]. A fully functional web-GIS application demonstrating the presented features is available at [i-mars.eu/web-gis](http://i-mars.eu/web-gis).

## Multi-temporal database

In order to locate multiple coverage of images and select images based on spatio-temporal queries, we converge available coverage catalogs for various NASA imaging missions into a relational database management system with geometry support. We harvest available metadata entries during our processing pipeline using the [Integrated Software for Imagers and Spectrometers \(ISIS\)](#) software. Currently, this database contains image outlines from the MGS/MOC, MRO/CTX and the MO/THEMIS instruments with imaging dates ranging from 1996 to the present. For the MEx/HRSC data, we already maintain a database which we automatically update with custom software based on the VICAR environment [6].

## Web Map Service with time support

The [MapServer](#) software is connected to the database and provides Web Map Services (WMS) with time support based on the START\_TIME image attribute. It allows temporal WMS-t GetMap requests by setting additional TIME parameter values in the request. The values for the parameter represent an interval defined by its lower and upper bounds. As the WMS time standard only supports one time variable, only the start times of the images are considered. Without time values submitted, the full time range of all images is assumed as the default.

## Dynamic single image WMS

To compare images from different acquisition times at sites of multiple coverage, we have to load every image as a single WMS layer. Due to the vast amount of single images we need a way to set up the layers in a dynamic way – the map server does not know the images to be served beforehand. We use the MapScript interface to dynamically access MapServer's objects and configure the file name and path of the requested image in the map configuration. The layers are created on-the-fly each representing only one single image. On the frontend side, the vendor-specific WMS request parameter "PRODUCTID" has to be appended to the regular set of WMS parameters. The request is then passed on to the MapScript instance.

## Web Map Tile Cache

In order to speed up access of the WMS requests, a [MapCache](#) instance has been integrated in the pipeline. For each image entity, a separate tile cache tree has to be generated. In this context the PRODUCTID parameter is configured as an additional dimension of the cache. The complete data flow of the described WMS request and its response is shown in Figure 1.

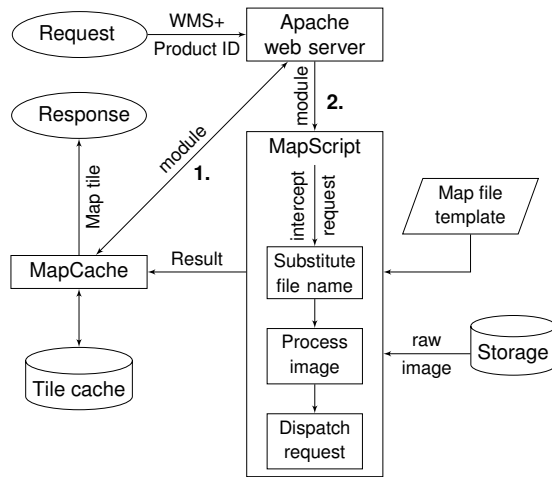


Figure 1: Diagram of the data workflow from the dynamic single-image WMS request to cache lookup to image processing and tile return. The numbers represent possible process paths as explained in the text.

The WMS request is received by the Apache web-server configured with the MapCache module. If the tile is available in the tile cache, it is immediately committed to the client (following path 1). If not available, the tile request is forwarded to Apache and the MapScript module (following path 2). The Python script intercepts the WMS request and extracts the product ID from the parameter chain. It loads the layer object from the map file and appends the file name and path of the inquired image. After some possible further image processing inside the script (e.g., stretching or colour matching), the request is submitted to the MapServer backend which in turn delivers the response back to the MapCache instance.

## Web frontend

We have implemented a web-GIS frontend based on various [OpenLayers](#) components. The basemap is a global colour-hillshaded HRSC bundle-adjusted DTM mosaic with a cell size of 50 m per pixel. The new bundle-block-adjusted quadrangle mosaics of the MC-11 quadrangle, both image [3] and DTM [4], are included with opacity slider options. The layer user interface has been adapted on the basis of the [ol3-layerswitcher](#) module and extended by foldable and switchable groups, layer sorting (by resolution, by time and alphabetically), layer deletion and reordering (drag-and-drop). A collapsible time panel accommodates a time slider interface where the user can filter

the visible data by a range of Mars or Earth dates. The visualisation of time-series of single images is controlled by a specific toolbar enabling the workflow of image selection, dynamic image loading and sequential playback of single images in a video player-like environment. We have also added a “Goto lat/lon” control to navigate in the map via text input, and a “Projection switcher” element for changing into polar stereographic projections. During a stress-test campaign we could demonstrate that the system is capable of serving up to 10 simultaneous users on its current lightweight development hardware.

## Conclusions/Outlook

We demonstrate a technique to dynamically retrieve and display single images based on the time-series structure of the data. Together with the multi-temporal database and its MapServer/MapCache backend it provides a stable and high performance environment for the dissemination of the various single image products. The web-GIS application serves as an expert tool for the detection and visualisation of surface changes in HRSC images.

## Acknowledgements

This research has received funding from the EU’s FP7 Programme under iMars 607379 and by the German Space Agency (DLR Bonn), grant 50 QM 1301 (HRSC on Mars Express).

## References

- [1] S. H. G. Walter et al., *LPSC*, 45, 2014, #1088.
- [2] J.-P. Muller et al., *ISPRS* 41B4 (2016), 453–458.
- [3] G. G. Michael et al., *PSS* 121 (2016), 18–26.
- [4] K. Gwinner et al., *PSS* 126 (2016), 93–138.
- [5] K. Gwinner et al., *EPSL* 294 (2010), 506–519.
- [6] S. H. G. Walter et al., *EPSC* 2006, 2006, #508.

## Semi-automated surface mapping via unsupervised classification

Mario D'Amore (1), Le Scaon (2), Jörn Helbert (1), Alessandro Maturilli (1)

(1) Institute for Planetary Research, DLR, Rutherfordstrasse 2, Berlin, Germany (mario.damore@dlr.de) (2) Ecole Polytechnique, Université Paris-Saclay, Paris, France

### Abstract

Due to the increasing volume of the returned data from space mission, the human search for correlation and identification of interesting features becomes more and more unfeasible. Statistical extraction of features via machine learning methods will increase the scientific output of remote sensing missions and aid the discovery of yet unknown feature hidden in dataset. Those methods exploit algorithm trained on features from multiple instrument, returning classification maps that explore intra-dataset correlation, allowing for the discovery of unknown features. We present two applications, one for Mercury and one for Vesta.

### 1. Introduction

Machine learning is a fast-growing subfield of computer science in which computers are

programmed to learn complex concepts and behaviours using generalized optimization procedures without being explicitly programmed. In recent years, machine-learning methods have achieved unprecedented results in image processing and other high-dimensional data processing tasks with wide applications from medical imaging and diagnosis to autonomous and assisted driving. ML is employed in a range of computing tasks where designing and programming explicit algorithms with good performance is difficult or unfeasible. Due to the growing number of complex nonlinear systems that have to be investigated in various fields of science and the bare raw size of data nowadays available, ML offers the unique ability to extract knowledge in an intelligible and innovate way regardless the specific application field. Examples are image segmentation, supervised/unsupervised/semi-supervised classification, feature extraction, data dimensionality analysis/reduction.

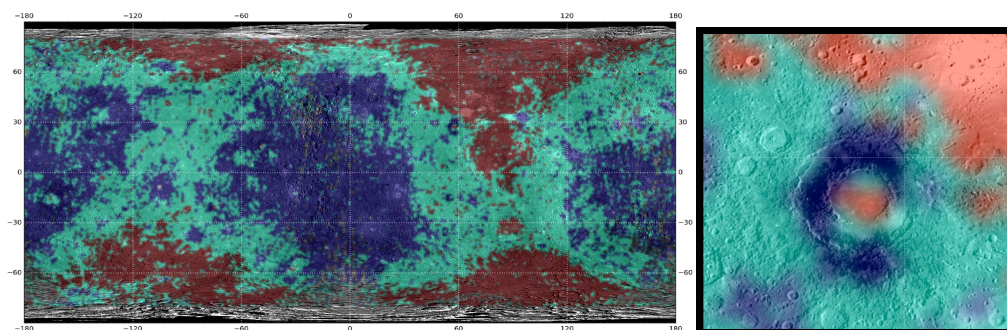


Figure 1: Classification on Mercury spectral data (left panel) in 3 classes. Zoom on Rachmaninoff with clear distinction inner and outer ring material from background material out of the crater.

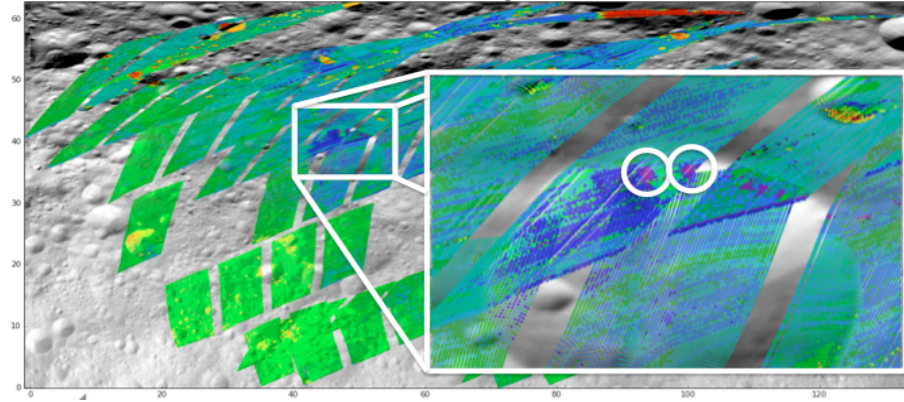


Figure 2: Automatic classification of DAWN/VIR spectral data. The two purple outcrops marked by circle on the crater wall correspond to the Olivine finding from [1].

## 2. Mercury Dataset

The Mercury Atmospheric and Surface Composition Spectrometer (MASCS) instrument has mapped Mercury surface in the 400–1145 nm wavelength range during orbital observations by the MESSENGER spacecraft. We have conducted k-means unsupervised hierarchical clustering to identify and characterize spectral units from MASCS observations. The results (Figure 1.) display a dichotomy, with two spectrally distinct groups: polar and equatorial units, possibly linked to compositional differences or weathering due to irradiation. To explore possible relations between composition and spectral behavior, we have compared the spectral provinces with elemental abundance maps derived from MESSENGER’s X-Ray Spectrometer (XRS). Nonetheless, by comparing the VIS/near-infrared MASCS and XRS datasets and investigating the links between them, we can provide further clues to the formation and evolution of Mercury’s crust.

## 3. Vesta Dataset

For the Vesta application, we explored several Machine Learning techniques: multi-step clustering method is developed, using an image segmentation method, a stream algorithm, and hierarchical

clustering. The DAWN Visible and infrared spectrometer (VIR) data from Vesta is are test-beds for our algorithm. The algorithm successfully separates the Olivine outcrops around two craters on Vesta’s surface [1]. New maps summarizing the spectral and chemical signature of the surface could be automatically produced.

## 4. Conclusion

The techniques applied belong to the vast file of ML and allow drastically reducing human time for the long data analysis work on bigger and bigger dataset. Instead of digging in single data-unit searching for novelties, scientist could choose a subset of algorithms with well known feature (i.e. efficacy on the particular problem, speed, accuracy) and focus their effort in understanding what important characteristic of the groups found in the data mean, their morphology on the surface and correlation with other datasets.

## References

- [1] E Ammannito et al. “Olivine in an unexpected location on Vesta’s surface”. In: *Nature* 504.7478 (2013), pp. 122–125.

## Stereo-Multispectral analysis of Phobos by using CaSSIS images

**Cristina Re (1)**, E. Simioni (1,2), G. Cremonese (1), A. Lucchetti (1), M. Pajola (3,1), A. Pommerol (4), N. Thomas (4)

(1) INAF, Osservatorio Astronomico di Padova, Italy (cristina.re@oapd.inaf.it); (2) CNR-Institute for Photonics and Nanotechnologies, Padova LUXOR, Padova, Italy (3) NASA Ames Research Center, Moffett Field, CA 94035, USA, (4) Physics Institute, Space Research and Planetary Sciences - University of Bern, Switzerland.

### 1. Introduction

The CaSSIS instrument (Colour and Stereo Surface Imaging System) [1], is the stereo imaging system onboard the European Space Agency's ExoMars Trace Gas Orbiter (TGO) that has been launched on 14 March 2016 and entered Mars orbit on 19 October 2016. During the first bounded orbits, CaSSIS acquired its first multiband images on 22 and 26 November 2016.

The system operates in "push-frame" mode and, differently by other Mars instruments with the same resolution [2], it provides images at different wavelengths thanks to a FSA (Filter Strip Assembly) with a panchromatic (PAN, centred at 675 nm) and 3 broadband colour filters within the visible range (the BLU filter being centred at 499 nm, the RED one at 836 nm and the NIR one centred at 937 nm). Furthermore, the CaSSIS instrument provides stereo pairs fundamental for the initialisation of the photogrammetric process to 3D reconstruct the Martian surface.

The availability of 3D data of a planetary surface enabled the morphological analysis of multiple features, providing a fundamental step forward for planetary geology. Indeed, enlarging the number of known details of the surface, allows a wider range of scientific investigation. Previous studies [3] reported that the use of chromatic information can significantly reduce the ambiguity between candidate matches of terrain features in the production of disparity maps between stereo image pairs. In this context, the CaSSIS multispectral images constitute an interesting dataset that allows the extraction of more accurate and detailed information. Therefore, a new approach in the stereo reconstruction pipeline is here proposed by taking advantage of the potentialities that can be obtained using CaSSIS multispectral data and, specifically, using Phobos images.

### 2. Phobos acquisitions of CaSSIS

On November 26, 2016, CaSSIS has imaged the Martian moon Phobos during the closest approach of the spacecraft around Mars at a distance of 7700 km. CaSSIS acquired a set of framelets in stereo mode with an average pixel scale of  $\sim 85$  m. The Phobos CaSSIS framelets in four different filters (0.499, 0.675, 0.836 and 0.937  $\mu\text{m}$ , [1]) have been mosaicked in order to provide the images (for each filter) of the entire shape of the satellite as shown in the Figure 1 (a). The mosaicking process has been performed through an algorithm that corrects the first solution provided by the SPICE kernels with a recursive process that implements the SURF (Speeded Up Robust Features) feature based operator [4].

### 3. New stereo approach for multispectral images

The common procedures based on automatic stereo image matching provide the so-called Digital Terrain Model (DTM). In the CaSSIS case study the stereo image processing should benefit from the usage of information coming from all bands contents. DTMs profiting from additional spectral input may have higher fidelity and resolution according to previous studies [5]. However, a direct assessment remains to be carried out for planetary surface images. The correlation based matching is the most common way to solve the point matching problems, however, it can introduce false matches (outliers), especially in regions lacking of both texture and information. These areas, which are very diffuse on the planetary surfaces (covered by regolith, smooth planes, poor in superficial variegation etc.), remain unsolved or low in accuracy after the matching process.



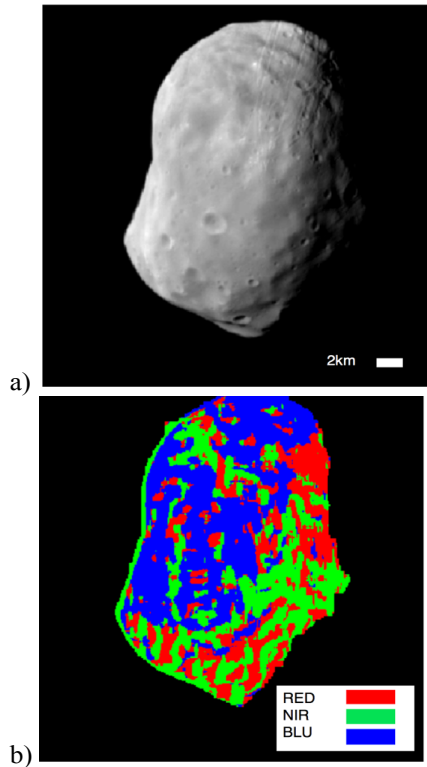


Fig. 1 a) Mosaicked image of Phobos using PAN filter acquisitions. b) Pixel identification as function of the best filter according to the higher local contrast (higher local standard deviation).

In this context, the idea proposed is to exploit the additional information coming from the spectral data in order to improve the performance of the common stereo PAN image matching, hence, providing more accurate and complete three-dimensional data. To achieve the goal, different areas have been identified on the image accordingly to the image content, which is evaluated by the local signal standard deviation ( $\sigma$ ) (mark of the local contrast). Firstly, for each filter, the corresponding points on the images are ordered into different areas as function of the degree of image content. Then, the matching algorithm can be addressed selecting the best image of a specific area. This choice is based on the observation that points of

larger gradient ( $\sigma$ ) have higher probability to be matched and, in addition, each filter is supposed to provide different content in relation with variations in perceived reflectance properties, even across smooth regions of dust [6]. Primarily, the procedure will foresee a previous analysis of the image quality by means of gradient intensity and image content indicators as the local standard deviations (Figure 1 (b)). Then, the DTM generation pipeline could be developed in multiple stages:

- 1) a matcher that takes one stereo pair (at a single wavelength) and produces a DTM;
- 2) combining multiple DTMs generated independently from different spectral wavebands;
- 3) employing “addressed”-correlation between the spectral wavebands.

Finally, the quality assessment of the results will be done in terms of coverage and accuracy. The impact of spectral data on the DTM production will be reported in comparison with results obtained through common panchromatic based DTM products.

## Acknowledgements

The authors wish to thank the spacecraft and instrument engineering teams for the successful completion of the instrument. CaSSIS is a project of the University of Bern and funded through the Swiss Space Office via ESA's PRODEX programme. The instrument hardware development was also supported by the Italian Space Agency (ASI) (ASI-INAF agreement no.2017-03-17), INAF/Astronomical Observatory of Padova, and the Space Research Center (CBK) in Warsaw. Support from SGF (Budapest), the University of Arizona (Lunar and Planetary Lab.) and NASA are also gratefully acknowledged

## References

- [1] Thomas, N. et al., 2016. 47th LPSC Congress, Abstract # 1306. [2] Malin, Michael C., et al. Journal of Geophysical Research: Planets 112.E5,2007. [3] Mühlmann et al., 2002, IJCV, 47(1):79–88 [4] Bay et al. Comput. Vision Image Und., 110, 3, 2008. [5] Bleyer and Chambon, 2010 and Galar et al., Optics Express 21 (1), 1247-1257, 2013. [6] Fernando et al., J Geophys. Res-Planets, 118(3), 2013.



# A review of Cartographic Symbol for Geologic and Geomorphologic Maps in Planetary Science

A. Naß (1), C.M. Fortezzo (2), J.A. Skinner Jr. (2), M.A. Hunter (2), and T.M. Hare (2)

(1) DLR, Institute for Planetary Research, Rutherfordstrasse 2, 12489 Berlin, Germany ([andrea.nass@dlr.de](mailto:andrea.nass@dlr.de)), (2) USGS Astrogeology Science Center, 2255 N. Gemini Drive, Flagstaff, Arizona

## Abstract

A critical review of existing standard for geological features in planetary sciences is important to ensure uniform and understandable maps in the future. This contribution presents current efforts to handle this within a joint USGS/ASC - DLR project.

## 1. Introduction

Maps are one of the most powerful communication tools for spatial data. Maps of planetary surfaces, in particular those of the Moon, Mars, and Venus, are standardized products and often prepared as a part of hypothesis-driven science investigations. The Planetary Geologic Mapping program, funded by NASA and coordinated by the USGS/ASC [1], produces high-quality, standardized, refereed geologic maps and digital databases of planetary bodies. In this context, 242 geologic/geomorphologic, and thematic map sheets and map series have been published since 1962. However, outside of this program, numerous non-USGS published maps are created as result of scientific investigations and published within peer-reviewed journal articles.

The mapping basis is mostly limited to remotely sensed satellite data, with a few exceptions from rover data. Furthermore, due to the complexity of planetary surfaces, diversity between different planet surfaces, and the varied resolution of the data, geomorphologic/geologic mapping is a challenging task and highly interpretative work.

Uniform and unambiguous data are fundamental to make quality observations that lead to unbiased and supported interpretations, especially when there is no current groundtruthing [2]. To allow for correlation between different map products (digital or analogue), the spatial objects are visualized by predefined and standardized cartographic symbols. [3] defines the most commonly used symbols, colours, and hatch patterns. Chapter 25 of this document defines the

Planetary Geology Features based on the symbols defined in [4].

The focus of this contribution is on changing the symbology with respect to time and how it effects communication within and between the maps. Two key questions are

*Q1* Does [3] provides enough variability within the chapter 25 and the other subcategories (e.g., faults) to represent the data within currently needed maps?

*Q2* What recommendations can the mapping community and its steering committees make to convey information succinctly and thoroughly in planetary themed maps to enhance a map's communicability?

## 2. Approach for

To determine the most representative symbol collection supporting future map results, we defined the task list as follows, we are currently working on:

*M1* Statistical review of existing symbol sets and collections: The symbol sets within the USGS products of the geologic mapping program (available here [1]) would be documented and analysed.

*M2* Establish a representative symbol set for planetary mapping: The results of M1 will be compared with the symbols in [3] to determine how they overlap. Finally, members of the mapping community and staff at USGS/ASC will review the symbols to identify where deficiencies and excesses exist within the current [3].

*M3* Update cartographic symbols: The symbol set resulting from M2 will be used to create a new set of symbols. This will respect symbols used in past maps, but will focus on retiring low-use and outmoded symbols and replacing them with the appropriate terrestrial symbols, when they exist.

*M4* Implementation into GIS-based mapping software: every particular (carto-)graphically formulated symbol will be implemented into the GIS software to increase the usability for the mappers.

This implementation will mimic the 2010 application of the planetary symbol set into ArcGIS ([5]), but also implementations into other GIS, e.g., QGIS.

*M5* Distribute the symbol set: to reach as many planetary users as possible, it is necessary to draw attention to the symbol recommendations (e.g. within workshop and conference contributions) and provide the updated symbol set at different locations (e.g., institute websites, cross link to international organizations like IAU, ICA, ISPRS, and initiatives like openplanetary [6], MAPSIT, FGDC, and academic institutes).

### 3. Current Status

We considered 154 of the 242 on [1] available geological maps sheets. Within these 154 maps the mappers used 531 different symbol descriptions (map legends have mean. = 12, max. = 30, and min. = 1 listed symbol). The symbol description often shows different phrasing for the same feature, so that the used description does often not link distinctively to one symbol graphic. Based on this fact, it isn't easily possible to find the most needed symbols. We generated an overview of the most described objects in a map by querying keywords in the statistic (see figure 1). This gives the first realistic hint to the most used objects which were described in the available maps and will serve as basis for the next decisions.

### 4. Summary and Outlook

Following the formulated task list, the next steps are:

- (1) Increase the statistical population by including representative maps in- and outside USGS maps.
- (2) Establish a digital collection of most used symbols for geological planetary maps.
- (3) Discuss colour recommendation for geological units of different planetary bodies and chronological epochs following, e.g. shown in [3] or [www.stratigraphy.org/](http://www.stratigraphy.org/).

After the first symbol collection a few more task are essential to enable a user-friendly and software independent usage of the symbols in GIS environment

*A1* merge symbols with predefined attribute values characterize planetary objects in geological data model – already ongoing approach see also [7].

*A2* convert and save symbols in open formats, e.g. \*.svg (already discussed in [5]).

A critical review of the existing standard for geological features in planetary sciences is important to ensure uniform and understandable maps in the future. Therefore we established the joint and ongoing project between USGS and DLR and are working on an updated symbol collection for geologic and geomorphologic maps.

If you as experienced mapper in planetary science like to volunteer, please contact us!

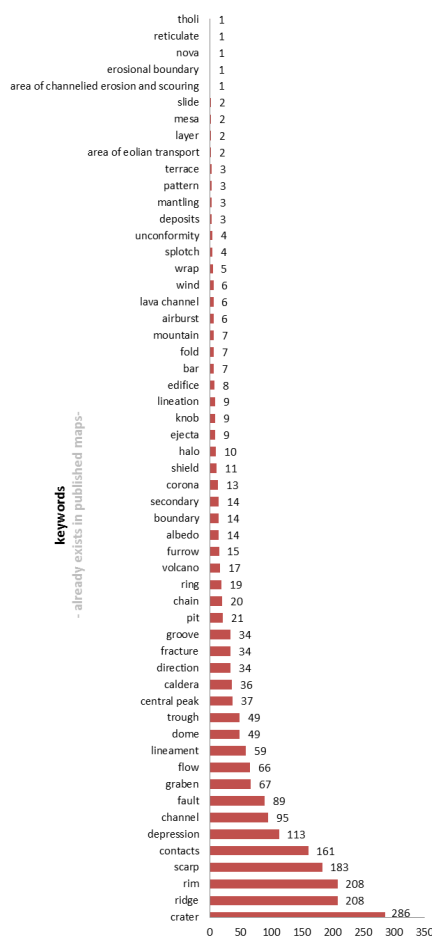


Figure 1 Statistical overview of already used symbol.

### References

- [1] United States Geological Survey, *Planetary Geologic Mapping Program Website*, <https://planetarymapping.wr.usgs.gov/>, 2016
- [2] Archinal et al., *LPSC*, #2286, 2017
- [3] FGDC, *Digital Cartographic Standard for Geologic Map Symbolization*, 2006
- [4] Tanaka, K. et al. *The Venus geologic mappers' handbook*, Open-File Report 94-438, U.S. Geological Survey, 1994
- [5] Naß, A. et al. *PSS*, Vol. 59(11-12), 2011
- [6] Manaud, N. et al., *DPS-EPSC*, #2587836, 2016,
- [7] Naß, A, *LPSC*, #1892, 2017.

# Merged data models for multi-parameterized querying: Spectral data base meets GIS-based map archive

A. Naß, M. D'Amore, and J. Helbert

Institute for Planetary Research, DLR, Rutherfordstrasse 2, Berlin, Germany (mario.damore@dlr.de, andrea.nass@dlr.de)

## Abstract

Current and upcoming planetary missions deliver a huge amount of different data (remote sensing data, in-situ data, and derived products). Within this contribution present how different data (bases) can be managed and merged, to enable multi-parameterized querying based on the constant spatial context.

## 1. Introduction

Since the 1990s, Europe has become highly active in planetary exploration with spacecraft contributions (e.g., Mars Express, Venus Express, Huygens probe, ExoMars, Rosetta), and employment of dedicated mapping instruments. Along with recent and upcoming missions also to Mercury (BepiColombo), the Outer Solar System moons (JUICE), and asteroids (NASA's Dawn mission), systematic mapping of surfaces has received new impulses. This systematic surface analysis based on comparison and combination of different remote sensing data sets, such as image data, spectral/hyperspectral sensor data, radar images, and/or derived products like digital terrain model. Conditioned by spatial component the derived information of such analysis mainly resulted in map figure, data, and project. Since the late 1990s the scientific mapping community has started to use Geographic Information Systems (GIS) for planetary mapping. GIS frameworks are usually based on databases which represent an ideal tool for generating, but also for archiving and storing spatial data - raster- as well as vector based data.

Within this contribution we discuss two questions:  
*Q1* How also planetary (vector-based) mapping data could be archived, thus they could finally be used as additional base data for further investigations?  
*Q2* How different mission data (base data and derived products listed above) could be merged, to generate combined querying for the most efficient data and information handling?

## 2. Current Framework

On the way to handle these two questions, we build upon two already existing developments, which are established within the Institute of Planetary Science, DLR.

*Part I:* The Planetary Spectroscopy Laboratory (PSL) group at DLR joins the Participating Scientists for MESSENGER program for the Mercury Atmospheric and Surface Composition Spectrometer (MASCS) instrument, allowing access to the team data before the official release to PDS. MASCS have mapped Mercury surface in the 400–1145 nm wavelength range during orbital observations by the MESSENGER spacecraft. To overcome the dataset bulk size and fully exploit the information present in it, we developed a PostgreSQL/PostGIS distributed database. The DB contains the whole MASCS spectral dataset, around 4 Millions single measurements as vector data, and user defined polygons. To explore possible relations between composition and spectral behaviour, we have imported other dataset, like the elemental abundance maps derived from MESSENGER's X-Ray Spectrometer (XRS).

*Part II:* In the last years the Department of Planetary Geology, DLR established a GIS-based mapping archive storing all different kind of derived vector-based mapping projects, which are conducting within different investigations. This data base driven archive has to cover the requirement, it is (1) applicable for all known planetary bodies, (2) usable in the proprietary environment ArcGIS™ (ESRI), but also usable and accessible within independent and open GIS systems, like e.g. QGIS, (3) developed, or at least transferable, into a PostgreSQL/PostGIS driven data base structure, and last but not least (4) the archived data should be available and replicable for future investigations. To accomplish these requirements, every dataset, has to be generated and described uniformly. Therefore, different recommendations are developed, and are used as reference, e.g. [1, 2]. One first implementation was

conducted for the systematic mapping of Ceres (Dawn mission), is useable also outside the DLR, and will be present on this conference [3].

### 3. Application

The current spatial intersection within Part I is a computation-heavy operation that is executed in the backend in period of low activity, typically at night. The current resulting features-measurements polygons intersection is stored in caching tables, allowing a quasi-live retrieve in GIS system from user perspective. The overhead in complexity is justified by the circumstance that the spatial query is executed only once, whereas the retrieving of the data could happen multiple times. Overall, despite the additional complexity and overhead to join different table, this approach optimizes the access time for spatial intersection. We are currently working on merging the GIS-based map archive to the PSL database to enable the data query for spectral data by the polygons, done within geologic/geomorphologic mapping projects.

### 4. Conclusion

The idea behind this contribution is to ingest the product of surface mapping done by experts (e.g., geomorphological or geological mapping), and

intersect those features with the actual data, to extract spectral information in well know geological regions (Figure 1). The ingestion architecture expects a minimum set of feature to be defined by the user. Three examples of this approach are: 1. the comparison spectral behaviour with radial distance in more than 100 craters on the surface of Mercury [4], 2. the identification of Olivine outcrops on the surface of Vesta via DAWN data analysis [5], 3. a general automated multi instrument mapping framework [6].

The current approach shows that databases described as *Part I* and *Part II* are (1) theoretically transferable to any planetary body, e.g. from Moon, Mars, (2) through the spatial context all these data hold by nature, the two parts are combinable, this (3) enables an overarching and comparative research and analysis basis by multi-parameterized querying, and would (4) benefits the knowledge management and data/product usability for future missions and data.

### References

- [1] Naß, A. et al., AutoCarto, 2010, [2] van Gasselt, S. & Naß, A., *PSS 59(11-12)*, 2011, [3] Naß, A., this issue, EPSC, 2017, [4] P. D'Incecco et al., *PSS 132(32-56)*, 2016, [5] D'Amore, M. et al, 48th LPSC, 2017, [6] D'Amore, M. et al. , EPSC 2017 (this conference), #497, 2017.

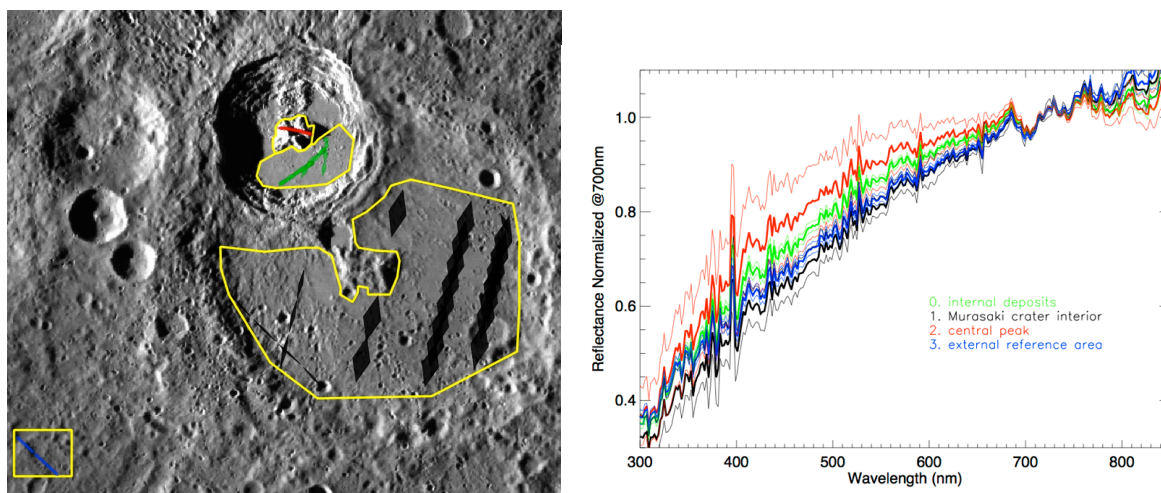


Figure 1: MASCS data coverage, incl. user defined area (right) and available spectral data (left) at Kuiper Crater (centered at 11.3 °S, 31.5°E), Mercury.

## SPICE for ESA Planetary Missions

M. Costa  
European Space Agency, ESAC – Cross Mission Support Office, Spain, (marc.costa@esa.int)

### Abstract

SPICE is an information system that provides the geometry needed to plan scientific observations and to analyze the obtained. The ESA SPICE Service generates the SPICE Kernel datasets for missions in all the active ESA Missions. This contribution describes the current status of the datasets, the extended services and the SPICE support provided to the ESA Planetary Missions (Mars-Express, ExoMars2016, BepiColombo, JUICE, Rosetta, Venus-Express and SMART-1) for the benefit of the science community.

### 1. Introduction

SPICE is an information system the purpose of which is to provide scientists the observation geometry needed to plan scientific observations and to analyze the data returned from those observations. SPICE is comprised of a suite of data files, usually called kernels, and software -mostly subroutines [1]. A customer incorporates a few of the subroutines into his/her own program that is built to read SPICE data and compute needed geometry parameters for whatever task is at hand. Examples of the geometry parameters typically computed are range or altitude, latitude and longitude, phase, incidence and emission angles, instrument pointing calculations, and reference frame and coordinate system conversions. SPICE is also very adept at time conversions.

### 2. The ESA SPICE Service

The ESA SPICE Service (ESS) leads the SPICE operations for ESA missions. The group generates the SPICE Kernel datasets for missions in operations (ExoMars 2016, Mars Express) missions in development (ExoMars RSP, BepiColombo, JUICE) and legacy missions (Rosetta, Venus Express). ESS is also responsible for the generation of SPICE Kernels for Solar Orbiter. The generation of these datasets includes the operation software to convert ESA orbit, attitude and spacecraft clock correlation data into the corresponding SPICE format. ESS also provides consultancy and support to the Science

Ground Segments of the planetary missions, the Instrument Teams and the science community. ESS works in partnership with NAIF.

### 3. Status of the Kernel Datasets

The current status of the SPICE Kernels datasets for the before mentioned missions will be described in this contribution. In general, the ESS is reviewing the legacy and operational datasets and is developing the ones for the future missions, the first reviews have shown that the Mars Express and Venus Express kernels need to be updated whereas the rest are in very good shape.

#### 3.1 SPICE Kernels Archived in the PSA

ESS is also responsible for the generation of PDS3 and PDS4 formatted SPICE Archives that are published by the PSA. ESS in close collaboration with NAIF peer-reviews the operational kernels for the PSA [2] to publish being compliant with the Planetary Data System (PDS) standards and uses them in the processes that require geometry computations [3].

### 4. Extended Services

The ESS offers other services beyond the SPICE Kernels datasets, such as configuration and instances for WebGeocalc and Cosmographia for the ESA Missions [4].

#### 4.1 SPICE-Enhanced Cosmographia

NAIF offers for public use a SPICE-enhanced version of the open source visualization tool named Cosmographia. This is an interactive tool used to produce 3D visualizations of planet ephemerides, sizes and shapes; spacecraft trajectories and orientations; and instrument field-of-views and footprints. ESS Service provides the setup in order to load the ESA Planetary Missions in Cosmographia, this contribution will demonstrate its usage within the ESA Planetary missions.



## 4.2 WebGeocalc

The WebGeocalc tool (WGC) provides a web-based graphical user interface to many of the observation geometry computations available from the "SPICE" system. A WGC user can perform SPICE computations without the need to write a program; the user need have only a computer with a standard web browser. WGC is provided to the ESS by NAIF. This contribution will outline the WGC instances for ESA Planetary missions.

## References

- [1] Acton C., Ancillary data services of NASA's Navigation and Ancillary Information Facility (1996), Planet. And Space Sci., 44, 65-70.
- [2] Bessel, S. et al., ESA's Planetary Science Archive: Preserve and Present Reliable Scientific Datasets (2017) Planet. And Space Sci. (submitted).
- [3] Besse, S. et al., The New Planetary Science Archive (PSA): Exploration and Discovery of Scientific Datasets from ESA's Planetary Missions (2017), Proceedings of the 3<sup>rd</sup> Planetary Data Workshop, Flagstaff, June 2017.
- [4] Acton, C. et al., A Look Towards the Future in the Handling of Space Science Mission Geometry (2017) Planet. And Space Sci (submitted).



# Automated dynamic feature tracking of RSLs on the Martian surface through HiRISE super-resolution restoration and 3D reconstruction techniques

Y. Tao, J.-P. Muller

Imaging group, Mullard Space Science Laboratory, University College London, Holmbury St Mary, RH5 6NT, UK  
([yu.tao@ucl.ac.uk](mailto:yu.tao@ucl.ac.uk); [j.muller@ucl.ac.uk](mailto:j.muller@ucl.ac.uk))

## Abstract

In this paper, we demonstrate novel Super-resolution restoration and 3D reconstruction tools developed within the EU FP7 projects and their applications to advanced dynamic feature tracking through HiRISE repeat stereo.

## 1. Introduction

Almost fifty years have elapsed since the NASA Mariner 4 spacecraft first took the pictures of the Martian surface. Over that time period, the resolution and quality of these images has improved from tens of kilometres up to 25 cm. Over the intervening  $\approx 50$  years, many areas on Mars have been imaged repeatedly more than 5 times for scientific studies.

Within the recently completed EU FP-7 iMars (<http://www.i-mars.eu>) project, a fully automated multi-resolution DTM processing chain was developed by UCL for NASA CTX and HiRISE stereo-pairs, called the Co-registration ASP-Gotcha Optimised (CASP-GO), based on the open source NASA Ames Stereo Pipeline (ASP) [1], tie-point based multi-resolution image co-registration [2], and the Gotcha [3] sub-pixel refinement method.

The implemented system guarantees global geo-referencing compliance with respect to High Resolution Stereo Colour imaging (HRSC), and hence to the Mars Orbiter Laser Altimeter (MOLA), providing refined stereo matching completeness and accuracy from the ASP normalised cross-correlation. In Parallel, a novel Super-resolution restoration (SRR) technique using Gotcha sub-pixel matching, orthorectification, segmentation, and 4<sup>th</sup> order PDE-TV, called GPT-SRR was developed [4]. SRR is able to restore 5cm-12.5cm near rover scale images (Navcam at a range of  $\geq 5$ m) from multi-angle repeat-pass 25cm resolution MRO HiRISE images [5].

## 2. Method

Recently, we explored the possibility to apply GPT-SRR on areas with known dynamic changes, including Recurring Slope Lineae (RSL), Gullies,

and Polar Dune Flows. The idea came about when observing individual input scenes for the 3 rovers and noting that the appearance of the rovers were different in each image but the final SRR image no longer included the rovers. Due to the ability of the SRR technique to extract super-resolution for static features, we are able to restore matched (unchanged) features and meanwhile automatically track the unmatched (dynamic) pixels to characterise and measure the “change”.

On the other hand, by adding 3D information from repeat DTMs produced from multiple overlapping stereo-pairs, we are able to restore the unchanged surface also in 3D as SRR requires multiple angle views as inputs. This allows us to overlay tracked dynamic features onto the reconstructed “original” surface, providing a much more comprehensive interpretation of the surface formation processes in 3D.

## 3. Results

In iMars,  $\sim 5,300$  CTX DTMs using the developed CASP-GO system. Around 400 HiRISE stereo pairs have 5 or more repeat views and these are being processed using the Amazon® AWS cloud computing resources that are all co-registered to a global reference system derived from MOLA.

In parallel, a recent study on one of the RSL sites (centre coordinates: 41.6°S, 202.3°E) in the Palikir Crater [6] took 8 repeat-pass 25cm HiRISE images from which a 5cm SRR image using GPT-SRR [Figure 1] was produced using SRR which is shown here in comparison with one of the original HiRISE images that have large RSL features [Figure 2]. The SRR image shows the restored static surface without any dynamic features. By tracking the unmatched features from the original HiRISE images, we are able to mask out the dynamic features (e.g. RSLs) on the static surface shown in [3].

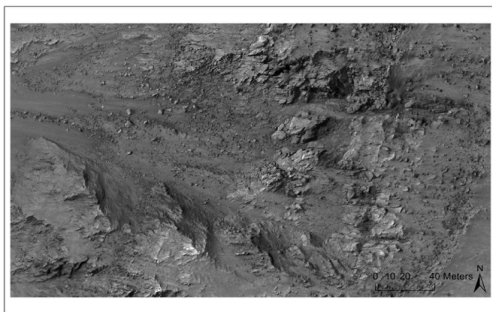


**Figure 1** Example of 5cm GPT-SRR image at Palikir Crater (centre coordinates: 41.6°S, 202.3°E) processed using 8 repeat-pass 25cm HiRISE images.

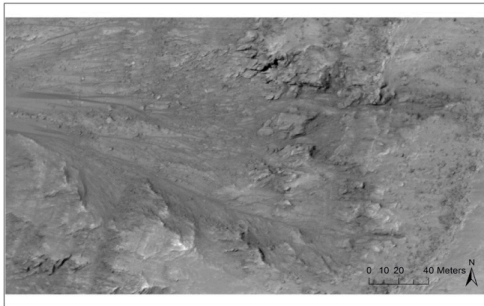


**Figure 2** Example of original 25cm HiRISE image (ESP\_031102\_1380) at Palikir Crater (centre coordinates: 41.6°S, 202.3°E) showing several (faint) RSL features.

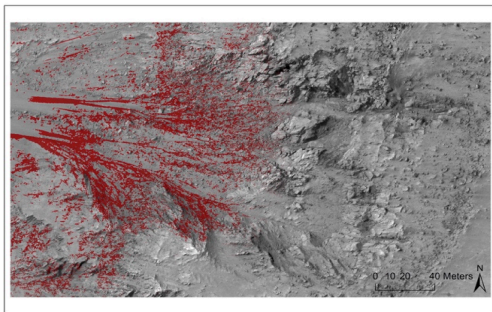


**Figure 3** Example of 5cm GPT-SRR image at Palikir Crater (centre coordinates: 41.6°S, 202.3°E) showing automatically tracked dynamic features (masked in red colour) from one of the original HiRISE scene (ESP\_031102\_1380).

## 4. Summary and Future work

This initial result shows only the total area that changed in 2D. It is planned to extend this to provide an index of individual features in HiRISE, image by image, and their associated velocities in 3D. This will enable better characterisation and modelling of dynamic features by analysing the “change-statistics”, including the total affected areas, shapes and propagation directions in 3D of the masked pixels. In addition, from the greater detail in the RSL-free image and DTM we are also able to observe fine-scale detail of the surface and detect if any small targets have moved as well as analyze their motion.

## Acknowledgements

The research leading to these results has received funding from the European Union's Seventh Framework Programme (FP7/2007-2013) under iMars grant agreement n° 607379 and from the STFC “MSSL Consolidated Grant under “Planetary Surface Data Mining” ST/K000977/1.

## References

- [1] Moratto, Z. M., M. J. Broxton, R. A. Beyer, M. Lundy, and K. Husmann, 2010. Ames Stereo Pipeline, NASA's Open Source Automated Stereogrammetry Software. Lunar and Planetary Science Conference 41, abstract #2364.
- [2] Y. Tao, J.-P. Muller, W. Poole (2016) Automated localisation of Mars rovers using co-registered HiRISE-CTX-HRSC orthorectified images and wide baseline Navcam orthorectified mosaics, ICARUS, Vol 280, p139-157.
- [3] Shin, D. and J.-P. Muller, Progressively weighted affine adaptive correlation matching for quasi-dense 3D reconstruction. Pattern Recognition, 2012. 45(10): p. 3795-3809.
- [4] Y. Tao and J.-P. Muller (2015) A novel method for surface exploration: super-resolution restoration of Mars repeat-pass orbital imagery, Planetary and Space Science, <http://www.sciencedirect.com/science/article/pii/S0032063315003591>.
- [5] Y. Tao and J.-P. Muller (2016), Quantitative assessment of a novel super-resolution restoration technique using HiRISE with Navcam images: how much resolution enhancement is possible from repeat-pass observations, ISPRS 2016 Commission IV, WG IV/8.
- [6] Massé, M., S. J. Conway, J. Gargani, and M. R. Patel (2016) “Transport processes induced by metastable boiling water under Martian surface conditions,” Nature, vol. 9, pp. 425–428, DOI: 10.1038/NGEO2706.

# Planetary science with the Large Binocular Telescope: Viewing the Solar System with a 23-meter aperture

A. Conrad and C. Veillet  
LBTO, University of Arizona USA

## Abstract

At the Nantes EPSC in 2011 we gave the first report of our plans to exploit the 23m aperture of the Large Binocular Telescope (LBT) to observe volcanoes on Io at M-band [1]. Then at the Nantes EPSC in 2015 we presented our completion of that effort [2] along with a progress report on three further analyses of that data collected during 2015, including an occultation of Loki by Europa. Here in section 1, we provide a progress report on those efforts which further exploit the 23m mode of LBT.

At the 2015 Nantes EPSC we also revealed plans to use a new multi-conjugate adaptive optics (MCAO) mode for observations of Jupiter's full disk. At that time the LBT MCAO System, LINC-NIRVANA [3]. In section 2 we report status and plans for that system, including a recent technical demonstration.

Lastly, in sections 3 and 4 we present two coming LBT facilities that will provide unique capabilities for studies in planetary science, binocular imaging and spectroscopy in un-phased, 12m mode for faint small bodies, and visible light AO for high resolution at shorter wavelengths.

## 1. Phased Binocular (23m mode)

In Fizeau 23 meter mode, LBT is capable of providing 100 km resolution on the surface of Io at M-band [2]. Now in a recent publication [4], this resolution has been improved by an order of magnitude. As reported in that publication, this LBT capability has lead to an understanding of the processes that result in varying, cyclic brightening episodes that have been observed, but not understood in depth until now.

## 2. Un-phased Binocular (12m mode)

On UT 18-Mar-2017 we observed with LBT 2016 HO3, earth's newest Quasi-satellite [5], and obtained

a light curve and visible wavelength spectra [6]. For both of these observations we obtained reasonable signal to noise of this faint object thanks to the collecting area of a 12-meter telescope (i.e., by combining the light from both LBT 8.4 meter mirrors, un-phased, in a seeing-limited mode).

## 3. MCAO (2x8m mode)

In 2008 Jupiter observations were taken with the MCAO demonstrator (MAD) system in 2008 [7]. Now, nearly 10 years later we are poised to improve on this demonstration using a permanent facility with a similar capability. In a technical demonstration on UT 30-March-2017 LINC-NIRVANA (L-N) [8], which is just beginning commissioning, demonstrated acquisition and closed loop AO with multiple stars; indicating that first light for this instrument, and then an observation of Jupiter's full disk, could take place as early as 2018.

## 4. Visible AO (8m mode)

Visible wavelength adaptive optics (Vis-AO), decreases the correctible wavelength from the current state of the art, H- & K-band (1.6 & 2.2 microns), to B- & R-band (0.4 & 0.7 microns). Visible-light AO observation of main belt asteroids (MBA) using the only currently productive visible light AO system [9] have showed promise. The Shark-Vis system [10] planned for LBT will provide sharper shape resolution via contours that has been possible to date (see figure x).

## 5. Conclusion

With more glass on a single mount, LBT provides unique capabilities for planetary science for both high angular resolution at infrared wavelengths now (including Fizeau interferometry for a 23m mode), and visible wavelengths in the near future. For faint objects, the un-phased mode yielding the collecting

area of a 12-meter telescope is useful for obtaining both light curves and spectra of small bodies.

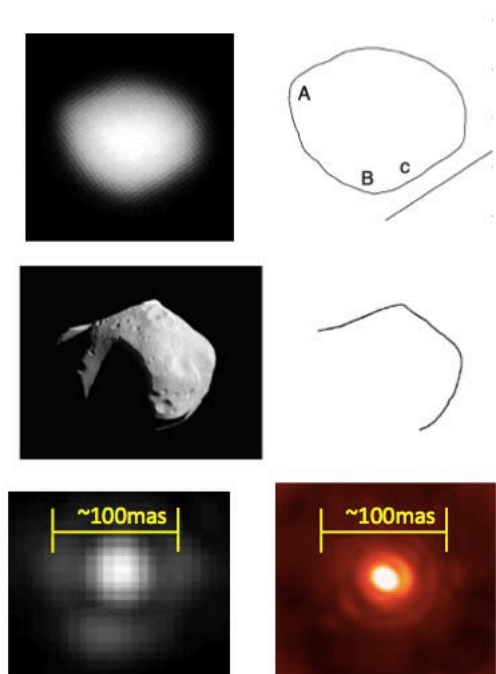


Figure 1. In this figure we show a sample image and its contour for (511) Davida from K-band imaging taken with a 10-meter telescope (first row), a figure from our 2007 analysis [11] posing the possibility of a large impact feature as seen in similar contours from spacecraft image of Mathilde (second row). With the improved resolution, as indicated by the respective PSF (third row), we hope to conclude whether or not this facet is a likely impact feature using the Shark-VIS system on LBT.

## References

- [1] Conrad, A., de Pater, I., Kürster, M., Herbst, T., Kaltenegger, L., Skrutskie, M., Hinz, P.: Observing Io at high resolution from the ground with LBT, EPSC-DPS Joint Meeting, 2011
- [2] Conrad, A., de Kleer, K., Leisenring, J., et al: Spatially Resolved M-band Emission from Io's Loki Patera – Fizeau Imaging at the 22.8 meter LBT, AJ, DOI:10.1088/0004-6256/149/5/175, 2015.
- [3] Herbst, T. M., Ragazzoni, R., Eckart, A., and Weigelt, G.: Imaging beyond the fringe: an update on the LINC-NIRVANA Fizeau interferometer for the LBT, SPIE 7734, 2010
- [4] de Kleer, I., et al: Multi-phase volcanic resurfacing at Io's Loki Patera, Nature, accepted, 2017
- [5] de la Fuente Marcos & de la Fuente Marcos, Asteroid (469219) 2016 HO3, the smallest and closest Earth quasi-satellite, MNRAS 462, 2016
- [6] Reddy et al., Physical properties of HO (2016), Icarus, in prep, 2017
- [7] Wong, M. H., Marchis, F., Marchetti, E., et al: A shift in Jupiter's equatorial haze distribution imaged with the Multi-Conjugate Adaptive Optics Demonstrator at the VLT, AAS/DPS, 2008
- [8] Herbst, T., et al., LN commissioning at LBT, Adaptive Optics for ELT 5, 2017
- [9] Shepard, M., et al, Radar observations and shape model of asteroid 16 Psyche, Icarus 281, 2017
- [10] Pedichini, F., et al, High-contrast imaging in the visible: First experimental results at the LBT, SPIE, 2016
- [11] Conrad et al, Direct measurement of shape and pole of (511) Davida taken in a single night, Icarus, 2007

# Mapping Lunar Impact Flashes

A. C. Cook (1), D. Thorpe (1), and M. D. Menzies (1)

(1) Department of Physics, Aberystwyth University, Aberystwyth, Ceredigion. SY23 3BZ. UK. (atc@aber.ac.uk)

## Abstract

Lunar Impact flashes are the result of the optical radiation of just under one percent of the kinetic energy released when meteoroids, travelling at tens of kilometres per second, strike the lunar surface. The locations of the impact sites of two photographic candidate impact flashes, are re-determined, and their apparent spatial extent given.

## 1. Introduction

Unless spacecraft images exist of the lunar surface, before and after a meteoroid strikes the Moon, and the images were taken under similar illumination angles, it is very difficult to identify which new crater has been formed amongst the already heavily cratered lunar surface [1]. This is furthermore hindered by Earth-based imagery being kilometre scale in resolution; whereas the resulting telescopic impact flash craters are on the scale of metres, i.e. a factor of a thousand times smaller. It is therefore essential to develop procedures which can narrow down the search space. We investigate a couple of historical observations of lunar flashes and simulate the visual appearance of the lunar terrain using the LDEM\_64 digital elevation model [2], with solar illumination and shadow effects added for the given date and UT of each flash.

## 2. Lunar Flare from: 1953 Nov 15

On this date at 02:00 UT Doctor Leon Stuart, of Tulsa, OK, USA, photographed a long duration flare (Fig 1 Left) apparently on the lunar surface which moved with the image of the Moon when he moved the telescope [3]. He took a photographic plate, went inside to develop it, and when he came back outside to observe later it had gone. One attempt has been made previously to locate the impact crater in modern era spacecraft imagery [4], however the location of the candidate craters has been shown to be incorrect [5]. Using the topocentric libration (sub-observer point), and sub-solar point, a computer

simulation was made to produce a virtual image of what the usual appearance surface of the Moon would have looked like (Fig 1 Centre). Using manually measured tie points, the image of the flash was affine transformed to the simulated view. From this we were able to determine the centre of figure of the flash lay at coordinates  $4.29^\circ$  N,  $3.30^\circ$  W, with an error of  $\pm 0.5$  km, based upon our uncertainty of measuring the positions of the tie points. This is illustrated in Fig 1-Right where the flash has been overlaid upon the simulation. The flash is circular, has a diameter of 35 km, and the area is  $\sim 974$  km<sup>2</sup>.



*Figure 1 The Pallas area of the Moon where in 1953 Nov 15 Leon Stuart photographed a lunar flare. (Left) Copy of the photographic plate taken by Leon Stuart. (Centre) An ALVIS simulation of the surface appearance. (Right) The flash photograph overlaid on the simulation.*

## 3. Lunar Flash from: 1985 May 23

On this date at 17:41 UT George Kolovos, was observing from a village in northern Greece (Nea Bafra, Serrai), capturing the Moon on 35 mm film. Without seeing it visually, he recorded a flash in the vicinity of Proclus C crater [6], however a later study [7,8] inferred that it may have come from a sun glint from a non-operational, rotating, US military DMSP F3 weather satellite, which was on a predicted track past the Moon. Subsequent correspondence suggested that sun-glint from solar panels (which are never perfectly optically flat) should have left a trail in the image [9]. As no trail was visible in the image another origin was suggested, namely a release of



light from piezoelectric effect [9, 10], when rocks fracture under thermal stress during sunrise. Alternatively, it was speculated that the flash resulted from a meteoroid impact on the Moon [11].

Using a similar approach to the 1953 flash, we produced a simulated view of the lunar surface and used this to refine the location of the flash (Fig 2). We deduce that the flash is an ellipse of  $a = 17.5$  km,  $b = 14.0$  km, and an area of  $\sim 770$  km<sup>2</sup>, as seen from Earth. Although the flash is slightly irregular in shape, in view of the photographic image noise, we do not see strong evidence that it may have illuminated surrounding terrain in the image [6], nor been modified in shape by the surrounding topography [9]. Neither do we see the semi-major axis of the flash lying along the trajectory of the satellite [7,8], which was aligned approximately 30° clockwise from the terminator at this location. We estimate the location of the flash as 13.40° N, 43.11° E  $\pm$  2.2 km in the image plane, based upon our tie point uncertainty.

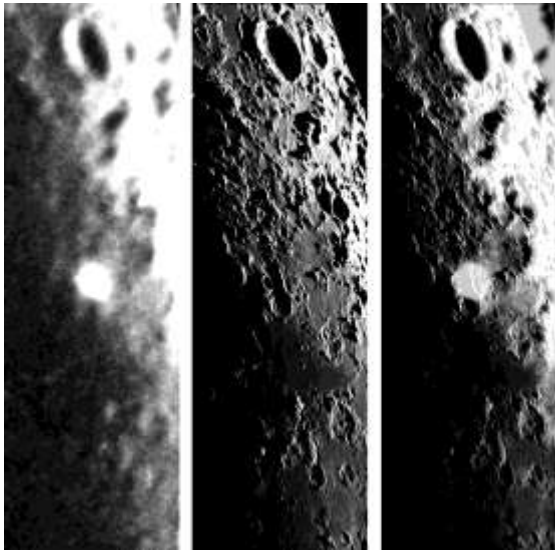


Figure 2: The 1985 May 23 observation of a flash on the Moon, by George Kolovos, Aristotle University of Thessaloniki, Greece. (Left) A scanned copy of the original image. (Centre) A computer simulation of the appearance of the lunar surface at the given date and time. (Right) Simulation with flash overlaid.

## 4. Discussion

The 1953 flare is widely regarded as the first known photographic record of an impact flash on the Moon and happened during the Leonid meteor shower. It

was also seen visually by the observer concerned on a photographic ground glass screen. By contrast the 1985 flash is less certain as it was not seen visually. Both flashes are not too dissimilar in apparent size.

It is important to note that the positions of the flashes found by ourselves have a caveat, namely it is assumed that the geocentric centre of each observed flash is the actual centre of the impact. Studies have suggested that this may not always be the case, in that there are at least three examples where supposedly point-like impact flashes, as videoed from Earth, have appeared elongated [11]. It is also possible that the area of each flash is the result of photographic halation and not a true spatial area on the Moon

We will refine our studies using a higher resolution DTM and allow for terrestrial atmospheric effects such as distortion due to atmospheric convection cells, and refraction, with the aim of reducing the measurement errors further. We have also been experimenting with the use of Earth-based imagery taken under similar illumination and viewing conditions, in order to better match the appearances of these historical observations than the simulations can provide.

## Acknowledgements

We would like to thank Jerry Stuart for supplying a scanned image of a copy of his father's photographic plate, and to George Kolovos for supplying some photographs of his recorded flash. Europlanet 2020 RI has received funding from the European Union's Horizon 2020 research and innovation programme under grant agreement No 654208 for the development of lunar impact flash detection software at Aberystwyth University.

## References

- [1] Speyer *et al.* *Nature*, 538, p215-218, 20. [2] Barker, M.K. *et al.*, *Icarus*, 273, p346-355, 2016. [3] Stuart, L.H., *The Journal of the International Lunar Society*, 1, p6-8, 1957. [4] Buratti, B.J. and Johnson, L.L., *Icarus* 161, p192-197. [5] Haas, W.H., *The Strolling Astronomer*, 47, p46-55, 2005. [6] Kolovos, G. *et al.*, *Icarus*, 76, p525-532, 1988. [7] Maley, P.D., *Icarus*, 90, p326-327. [8] Rast, R.H., *Icarus*, 90, p328-329, 1991. [9] Kolovos, G. *et al.*, *Icarus*, 97, p142-144, 1992. [10] Zitto, R.R., *Icarus*, 92, p419-422, 1989. [11] Madieto, J.M. *et al.*, *Astronomy and Astrophysics*, A118, p1-9, 2015. [12] Menzies *et al.* (This conference). 2017.



# Inter-comparison of Methods for Extracting Subsurface Layers from SHARAD Radargrams over Martian polar regions

S. Xiong (1) J.-P. Muller (1) and R. C. Carretero (1,2)

(1) Imaging Group, Mullard Space Science Laboratory, University College London, Holmbury St. Mary, Dorking, Surrey, RH5 6NT, UK, (2) Universidad Pontificia Comillas, Madrid, Spain. ([siting.xiong.14@ucl.ac.uk](mailto:siting.xiong.14@ucl.ac.uk))

## Abstract

Subsurface layers are preserved in the polar regions on Mars, representing a record of past climate changes on Mars. Orbital radar instruments, such as the Mars Advanced Radar for Subsurface and Ionosphere Sounding (MARSIS) onboard ESA Mars Express (MEX) and the SHallow RADar (SHARAD) onboard the Mars Reconnaissance Orbiter (MRO), transmit radar signals to Mars and receive a set of return signals from these subsurface regions. Layering is a prominent subsurface feature, which has been revealed by both MARSIS and SHARAD radargrams over both polar regions on Mars. Automatic extraction of these subsurface layering is becoming increasingly important as there is now over ten years' of data archived. In this study, we investigate two different methods for extracting these subsurface layers from SHARAD data and compare the results against delineated layers derived manually to validate which methods is better for extracting these layers automatically.

## 1. Introduction

Aside from surface images, radar sounding provides a non-intrusive and relatively direct way to investigate the structure and dielectric characteristics of the subsurface. Radar sounders operate at low frequency (several megahertz to hundreds of megahertz), and transmit waves into the subsurface and record the signals scattered back from subsurface structures and dielectric discontinuities [1]. The orbital images collected by these radar sounders are called radargrams which are formed by sets of radar return signals reflected from subsurface features as the platform moves forward in its orbit. Therefore, a radargram shows a sounding profile taken over a certain ground track.

Subsurface layers of PLDs have been revealed by the MARSIS and SHARAD [2-3]. These two instruments are currently orbiting around Mars and provide high-quality data which make a detailed study of the subsurface of Mars possible. Compared to MARSIS, SHARAD provides radargrams of higher range (vertical) resolution, which is 15 m in free space and 10 m within ice [3]. This makes it possible to detect fine linear interfaces in the Polar Layer Deposits (PLDs).

MARSIS and SHARAD have been orbiting Mars and collecting a huge amount of data for more than ten years.

However, the analysis of such data has been carried out mainly by means of manual investigation, especially in the case of these planetary missions. The huge data collection calls for the development of automatic or semi-automatic techniques for the analysis of radar sounder data in order to extract this geometric information from the radargrams in an effective and fast way. Extracting subsurface layers from radargrams is a preliminary step before trying to connect these layers to other geological knowledge. Thus, the development of automatic techniques for the analysis of these radargrams is of fundamental importance for full data exploitation.

In this study, we developed two methods for detecting subsurface linear features from SHARAD radargrams, one of which is based on a Continuous Wavelet Transform (CWT) and Hough line detection, the other is based on an event detection algorithm, which itself is based on signal analysis by a short-term-average/long-term-average (STA/LTA) phase picker taken along a characteristic function. Radargrams from both NPLD and SPLD are used to validate the effectiveness of the proposed methods. To validate the results, we manually delineate subsurface layers from the radargrams and then compare the results with the manually delineated layers.

## 2. Datasets and Methods

The SHARAD radar sounder is provided by the Agenzia Spaziale Italiana (ASI). The characteristics of this radar sounder can be found in [4]. The spatial resolution of the radargrams is approximately  $450 \text{ m} \times 3 \text{ km}$  (along track  $\times$  across track). The range sampling is 37.5 ns, corresponding to 5.63 m in free space and slightly more than 3 m in an icy subsurface ( $\epsilon = 3.15$ ). The range resolution is 10 m in ice.

In this study, extraction of layering features from radargram is separated into three steps. Firstly, we apply an image enhancement by using log-Gabor filtering to the original radargram to denoise the image. Secondly, along each columns (profile) of the radargram, we apply two different methods to extract the peaks of signal, which indicate the dielectric contrasts. The first method is based on Continuous wavelet, through which the signal can be analysed at different scales,  $s = \{1, 2, 3, \dots, N\}$ . After the derivation of the scalogram, we can extract the stable peaks which show high signal at different scales. The second method is an event detection algorithm, which is based on signal analysis by a short-term-average/long-term-average

(STA/LTA) phase picker taken along a characteristic function. Finally, a Hough Line Detection (HLD) is applied to the extracted peaks to connect the peaks into line segments.

### 3. Results

The proposed processing flow is here applied to four radargrams in the Martian polar regions. Currently, an example of the results from one SHARAD radargram (product ID: s\_00598301) is shown in Figure 1.

### 4. Discussion and Conclusions

In this study, we proposed two methods to extract subsurface layering features from SHARAD radargrams. From the preliminary results, we can see that by using CWT, more peak signals in the radargram have been picked out than those from the event detection algorithm, in which a number of peaks is largely dependent on the window selection. In this example, the selected window size tends to choose a moderate number of peaks to depress the background noise signal. On the other hand, the CWT tends to pick out more signal peaks, and in the following HLD, the peaks can be connected, while scattered background noise is depressed. The HLD results in long continuous lines when there are more peaks which belong to the same layer have been detected. However, when a smaller number of peak signals have been detected, then it results in short segmented lines.

### Acknowledgements

Part of the research leading to these results has received funding from the STFC “MSSL Consolidated Grant” ST/K000977/1 and partial support from the European Union’s Seventh Framework Programme (FP7/2007–2013) under iMars grant agreement No. 607379 as well as from the China Scholarship Council and the UCL Dean of MAPS fund.

### References

- [1] Ferro, A., and Bruzzone, L. Automatic Extraction and Analysis of Ice Layering in Radar Sounder Data. *IEEE Transactions on Geoscience and Remote Sensing*, 51, 1622–1634, 2013. doi:10.1109/TGRS.2012.2206078.
- [2] Picardi, G., Biccari, D., Seu, R., et al. MARSIS: Mars Advanced Radar for Subsurface and Ionospheric Sounding. *European Space Agency ESA SP (1291): 97–114*, 2009.
- [3] Iamini, E., Fois, F., Calabrese, D., et al. Sounding Mars with SHARAD & MARSIS. In *Proceedings of the 2007 4th International Workshop on Advanced Ground Penetrating Radar, IWAGPR*, 2007. doi:10.1109/AGPR.2007.386561.

- [4] Seu, R., Roger, J. P., Biccari, D., et al. SHARAD Sounding Radar on the Mars Reconnaissance Orbiter. *Journal of Geophysical Research: Planets* (1991–2012) 112 (E5): 1–18, 2007.

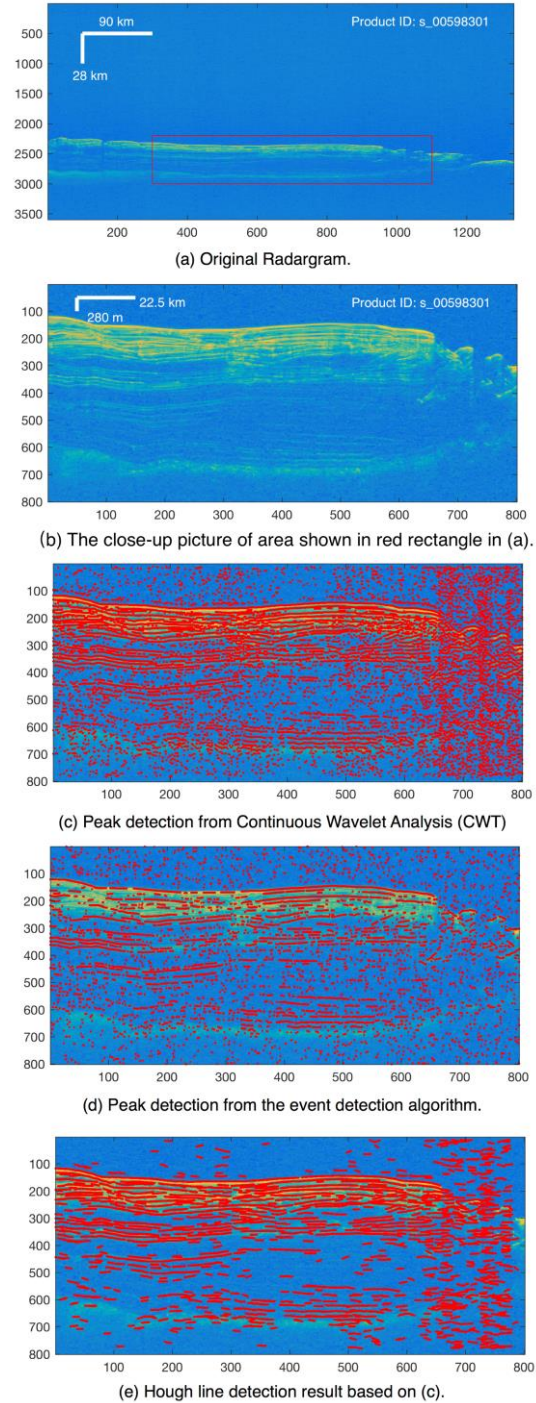


Figure 1. Preliminary results from CWT + HLD, and an event detection algorithm with short-term window of 9 pixels and long-term window of 13 pixels (the vertical scale bar in (a) and (b) is in the free space).

# Hyperspectral characterisation of the Martian south polar residual cap using CRISM

Jacqueline D. Campbell, Panagiotis Sidiropoulos and J-P. Muller.

Imaging Group, Mullard Space Science Laboratory, University College London, Holmbury St Mary, Surrey, RH5 6NT, UK

## Abstract

We present our research on hyperspectral characterization of the Martian South Polar Residual Cap (SPRC), with a focus on the detection of organic signatures within the dust content of the ice. The SPRC exhibits unique CO<sub>2</sub> ice sublimation features known colloquially as ‘Swiss Cheese Terrain’ (SCT). These flat floored, circular depressions are highly dynamic, and may expose dust particles previously trapped within the ice in the depression walls and partially on the floors. Here we identify suitable regions for potential dust exposure on the SPRC, and utilise data from the Compact Reconnaissance Imaging Spectrometer for Mars (CRISM) on board NASA’s Mars Reconnaissance Orbiter (MRO) satellite to examine infrared spectra of dark regions to establish their mineral composition, to eliminate the effects of ices on sub-pixel dusty features, and to assess whether there might be signatures indicative of Polycyclic Aromatic Hydrocarbons (PAHs). Spectral mapping has identified compositional differences between depression rims and the majority of the SPRC and CRISM spectra have been corrected to minimise the influence of CO<sub>2</sub> and H<sub>2</sub>O ice. Whilst no conclusive evidence for PAHs has been found, depression rims are shown to have higher water content than regions of featureless ice, and there are indications of magnesium carbonate within the dark, dusty regions.

## 1. Introduction

While Mars was initially not thought to have been a planet with a dynamic surface, repeat observations starting with the Mariner missions of the 1960s [1] have indicated otherwise. In particular, the polar caps exhibit significant change over time, both seasonal and long term. On board MRO is an imaging spectrometer, CRISM [2] attaining spatial resolutions of  $\approx 20\text{m}$  and spectral resolutions of 6nm, which can analyse compositional properties of the Martian surface. Mars’ south polar cap consists of a

permanent 400km diameter layer of solid CO<sub>2</sub>, 8m thick, overlaying water ice [3].

Swiss Cheese Terrain (SCT) is a unique surface feature found only in the SPRC. Its characteristic appearance (shown in Figure 1) is thought to be caused by seasonal differences in the sublimation rates of water and CO<sub>2</sub> ice [4]; scarp retreat through sublimation may expose dust particles previously trapped in the SPRC which can then be analysed using CRISM.

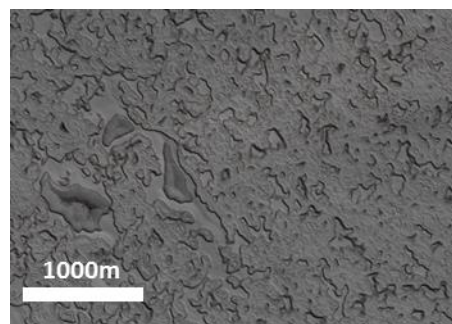


Figure 1: SCT sublimation features (CTX: B08\_012572\_0943\_XI)

## 1.1 Polycyclic Aromatic Hydrocarbons

PAHs are a group of chemical compounds consisting of benzene rings of hydrogen and carbon [5] and are considered to be important in theories of abiogenesis; the search for organic molecules on Mars is important in ascertaining Mars’ past conditions, and current habitability [6].

PAHs are abundant throughout the universe, and have been found to coalesce in space within dust clouds, [7] and have been detected on two of Saturn’s icy moons, Iapetus and Phoebe [8]. The delivery of complex organic compounds to established, habitable planets via bolide impact is a very important concept in astrobiology. The ability to identify PAHs could



prove a critical tool in the search for putative locations for extra-terrestrial organisms.

To date, the hypothesised connection of Martian Swiss Cheese Terrain and the presence of PAHs has not been systematically examined.

## 2. Methods

Initially only Full Targeted Resolution (FRT) CRISM products have been considered for study to try to maximise spatial resolution (~20m/pixel) of small-scale features. Analysis of the SPRC has been carried out using HiRISE, CTX, MOC-NA and HRSC imagery to better constrain regions of interest, and select CRISM scenes for spectral analysis. 72 FRT CRISM scenes were identified as containing SCT; these were arranged into groups of stacked images, resulting in 13 stacks each containing several FRT scenes taken over a period of 3 Martian years, totalling 55 images, which could then be examined for temporal and spatial spectral changes.

The CRISM Analysis Tool (CAT) plugin for ENVI software was used to process the 55 CRISM scenes with corrections for photometry, atmosphere, image artefacts, ‘despiking’ and ‘destriping’, and to generate summary products. 44 spectral summary products based on multispectral parameters are derived from reflectances for each CRISM observation that can be used as a targeting tool to identify areas of mineralogical interest for further analysis [9]. Those of particular interest to this investigation are those which highlight carbonate overtones, and CO<sub>2</sub> and water ice, in order to differentiate materials of astrobiological interest from the bulk of the SPRC.

Pelkey’s summary products were utilized to create RGB composite images of regions of interest to identify regions of spectral difference around dust rims (figure 2).

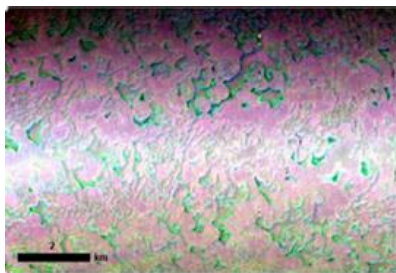


Figure 2: False colour visualization of CRISM scene 00005D24. Red: CO<sub>2</sub> ice, Green: H<sub>2</sub>O ice, Blue: carbonate over-tones

## 3. Conclusions

There are clear spectral differences between dust rims and non-rim regions, with indications of carbonate components within SCT dust rims. CO<sub>2</sub> ice signatures are a limiting factor in identifying PAHs as the removal of CO<sub>2</sub> ice spectrum may also remove subtle features in the 3.3µm region of CRISM spectra. Work is currently being carried out to look for compositional changes over time in dust-rich regions, and how spectral changes relate to dust content and morphological processes.

## Acknowledgements

The research leading to these results has received partial funding from the STFC “MSSL Consolidated Grant” ST/K000977/1 and partial support from the European Union’s Seventh Framework Programme (FP7/2007-2013) under iMars grant agreement n° 607379 and the first author is supported by STFC under PhD studentship no. 526933.

## References

- [1] NASA (2015) <http://science.nasa.gov/missions/marinermissions>
- [2] Murchie et al. (2007) JGR, doi:10.1029/2006JE002682
- [3] Vita-Finzi, C. (2005) Planetary Geology, 146-159.
- [4] Tokar et al., (2003) GRL, 30, 1677, 13.
- [5] Carey, F.A. Organic Chemistry, 398-423 [7] Vita-Finzi, C. (2005) Planetary Geology, 146-159.
- [6] Benner, S.A. et al. (1998) PNAS, 96,6,2425-2430
- [7] Allamandola, L.J. (2011) EAS, 46,305-317
- [8] Cruikshank, D.P. et al. (2008) Icarus, 193, 334-343
- [9] Pelkey, S.M. et al. (2007) JGR, doi:10.1029/2006JE002831